AGU PUBLICATIONS

Paleoceanography

RESEARCH ARTICLE
10.1002/2017PA003203

**Key Points:**
- Coral SST reconstruction (1578–2009) for subtropical western North Pacific
- Proxy for Western Pacific teleconnection pattern
- Record of "Little Ice Age" in South Japan

**Supporting Information:**
- Supporting Information S1
- Table S1

**Correspondence to:**
C. Alibert,
c.alibert@anu.edu.au

**Citation:**
Kawakubo, Y., Alibert, C., & Yokoyama, Y. (2017). A reconstruction of subtropical western North Pacific SST variability back to 1578, based on a *Porites* Coral Sr/Ca record from the northern Ryukyus, Japan. *Paleoceanography*, *32*, 1352–1370. https://doi.org/10.1002/2017PA003203

Received 3 JUL 2017
Accepted 10 NOV 2017
Accepted article online 15 NOV 2017
Published online 7 DEC 2017



# A Reconstruction of Subtropical Western North Pacific SST Variability Back to 1578, Based on a *Porites* Coral Sr/Ca Record from the Northern Ryukyus, Japan

**Y. Kawakubo[1], C. Alibert[2], and Y. Yokoyama[1]**

[1]Atmosphere and Ocean Research Institute, University of Tokyo, Kashiwanoha, Japan, [2]Research School of Earth Sciences, Australian National University, Canberra, ACT, Australia

**Abstract** We present a seasonal reconstruction of sea surface temperature (SST) from 1578 to 2008, based on a *Porites* coral Sr/Ca record from the northern Ryukyus, within the Kuroshio southern recirculation gyre. Interannual SST anomalies are generally ~0.5°C, making Sr/Ca-derived SST reconstructions a challenging task. Replicate measurements along adjacent coral growth axes, enabled by the laser ablation inductively coupled plasma mass spectrometry technique used here, give evidence of rather large uncertainties. Nonetheless, derived winter SST anomalies are significantly correlated with the Western Pacific atmospheric pattern which has a dominant influence on winter temperature in East Asia. Annual mean SSTs show interdecadal variations, notably cold intervals between 1670 and 1700 during the Maunder Minimum (MM) and between 1766 and 1788 characterized by a negative phase of the North Atlantic Oscillation. Cold summers in 1783 and 1784 coincide with the long-lasting Laki eruption that had a profound impact on the Northern Hemisphere climate, including the severe "Tenmei" famine in Japan. The decades between 1855 and 1900 are significantly cooler than the first half of the twentieth century, while those between 1700 and 1765, following the MM, are warmer than average. SST variability in the Ryukyus is only marginally influenced by the Pacific Decadal Oscillation, so that external forcing remains the main driver of low-frequency temperature changes. However, the close connection between the Kuroshio extension (KE) and its recirculation gyre suggests that decadal SST anomalies associated with the KE front also impact the Ryukyus, and there is a possible additional role for feedback of the Kuroshio-Oyashio variability to the large-scale atmosphere at decadal timescale.

## 1. Introduction

Analyses of coral skeletal aragonite for Sr/Ca and oxygen isotopic composition have been widely used since the early 1990s to reconstruct past tropical climate variability (e.g., Tierney et al., 2015; Urban et al., 2000, and references therein), but only a few monthly or seasonally resolved records extend over 200 years (e.g., Asami et al., 2005; DeLong et al., 2012, 2014). In Japan, the few climate proxies that cover the Little Ice Age (LIA, circa 1550–1700), during which cooling was driven by low solar irradiance, reduced insolation, and stratospheric aerosols from volcanic eruptions (e.g., Ammann et al., 2007), consist of historical documents (Mikami, 2008) and temperature/precipitation tree ring reconstructions for the spring/summer season (Cook et al., 2012; D'Arrigo & Wilson, 2006; D'Arrigo et al., 2014; Ohyama et al., 2013; Sakashita et al., 2016; Yamaguchi et al., 2010). Although the impact of the solar cycle on the global climate is small (Schurer et al., 2014), an amplified regional response to the variability in ultraviolet solar irradiance through atmospheric teleconnections is now widely accepted (e.g., Meehl et al., 2009). Marine proxy records from the subtropical North Pacific ocean are therefore of great interest to better understand how solar forcing affects sea surface temperature (SST) spatial patterns during the LIA and more generally to document decadal climate variability in South Japan during the preindustrial era, in particular for the boreal winter season not covered by tree ring archives.

We present here an exceptionally long reconstruction of SST back to 1578, based on high-resolution Sr/Ca measurements by laser ablation inductively coupled plasma mass spectrometry (ICP-MS) of a massive *Porites* coral from Kikai, a small island of the northern Ryukyus (Figure 1). Fringing coral reefs owe their presence at this relatively high latitude (28°–30°N) to the warm waters conveyed by the Kuroshio (e.g., Hu et al., 2015). As a result, the average winter water temperature is ~20°C around Kikai Island. This region is part of the Kuroshio southern recirculation gyre where SST variations are influenced by both oceanic and atmospheric processes, in a similar way as shown for the Kuroshio extension (KE) region by Qiu (2000). The decadal KE

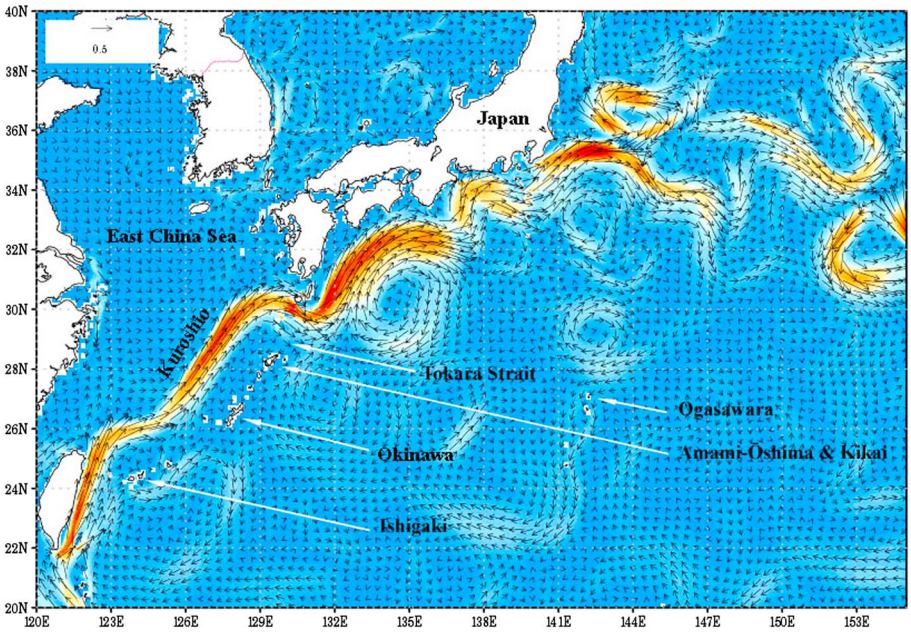


**Figure 1.** The Ryukyu Arc stretches ~1,000 km southwestward from Kyushu to Taiwan. The coral was collected on the south coast of Kikai (also known as Kikaijima), a small island 40 km east of Amami-Ōshima. These two islands are part of the Amami Group, the northernmost part of the Ryukyus. The Kuroshio exits the East China Sea through the Tokara Strait ~150 km to the north of Kikai Island. This map from the JAMSTEC/JCOPE website (http://www.jamstec.go.jp/jcope/vwp/) shows surface current velocities for 15 February 2007 (FRA-JCOPE2 daily reanalysis). The highest values around 1.1 m/s (dark orange) trace the path of the Kuroshio which separates from the coast of Japan near 35°N and 140°E to form the Kuroshio extension (KE) and its southern recirculation gyre. These are associated with mesoscale eddies; for example, a large anticyclonic (warm) eddy can be seen east of the Ryukyus between Kikai and Okinawa.

variability is largely a lagged response to wind forcing over the midlatitude North Pacific Ocean (Qiu & Chen, 2010). In the Ryukyu region, SST is strongly influenced by the large-scale atmospheric circulation at the interannual timescale, as expected for the extratropical North Pacific (Davis, 1976).

## 2. Key Controls on Regional SST and Nonseasonal SST Variability

An account of the climate in the Ryukyus and the sources for the climate data used here are given as supporting information.

### 2.1. The Oceanic Forcing

The 1-point correlation map of SST anomalies between Kikai and the northwest Pacific (Figure 2a) shows similar variability for the entire region of the Ryukyus between 25° and 30°N, extending eastward toward the southern recirculation gyre during winter. As a result, SST anomalies around Kikai are correlated with those in the KE region (34°–36°N, 140°–154°E) but only in winter ($r$ = 0.63, supporting information Table S1). Anticyclonic eddies detected from satellite-derived sea surface height (SSH) (supporting information Figure S2) are associated with positive SST anomalies. The typical size of these eddies, of the order of 100 km (Figure 1), can account for small differences of temperature between the northern and southern Ryukyu Islands. However, high-resolution daily SST maps (see online maps at http://www.esrl.noaa.gov/psd/) indicate that while large SST and SSH anomalies are found in the East China Sea and along the meandering Kuroshio south of Japan, eddy-related SST anomalies are generally less than 0.5°C in the northern Ryukyus. Accordingly, a map of the standard deviation ($\sigma$) of the monthly SST anomaly using 1° gridded data (Figure 2b) resolves the large anomalies $>$1°C along the KE but shows lesser variability along the Ryukyus (~0.5°C). Furthermore, the interannual variations of transport for the Ryukyu Current System, east of Amami-Ōshima, between 1993 and 2012 (Thoppil et al., 2016) are not clearly correlated with SSTs around Kikai. One exception was after the very strong El Niño 1997/1998 when strong current transport coincided with the arrival of anticyclonic eddies originating from the Kuroshio recirculation. Similarly, high SST

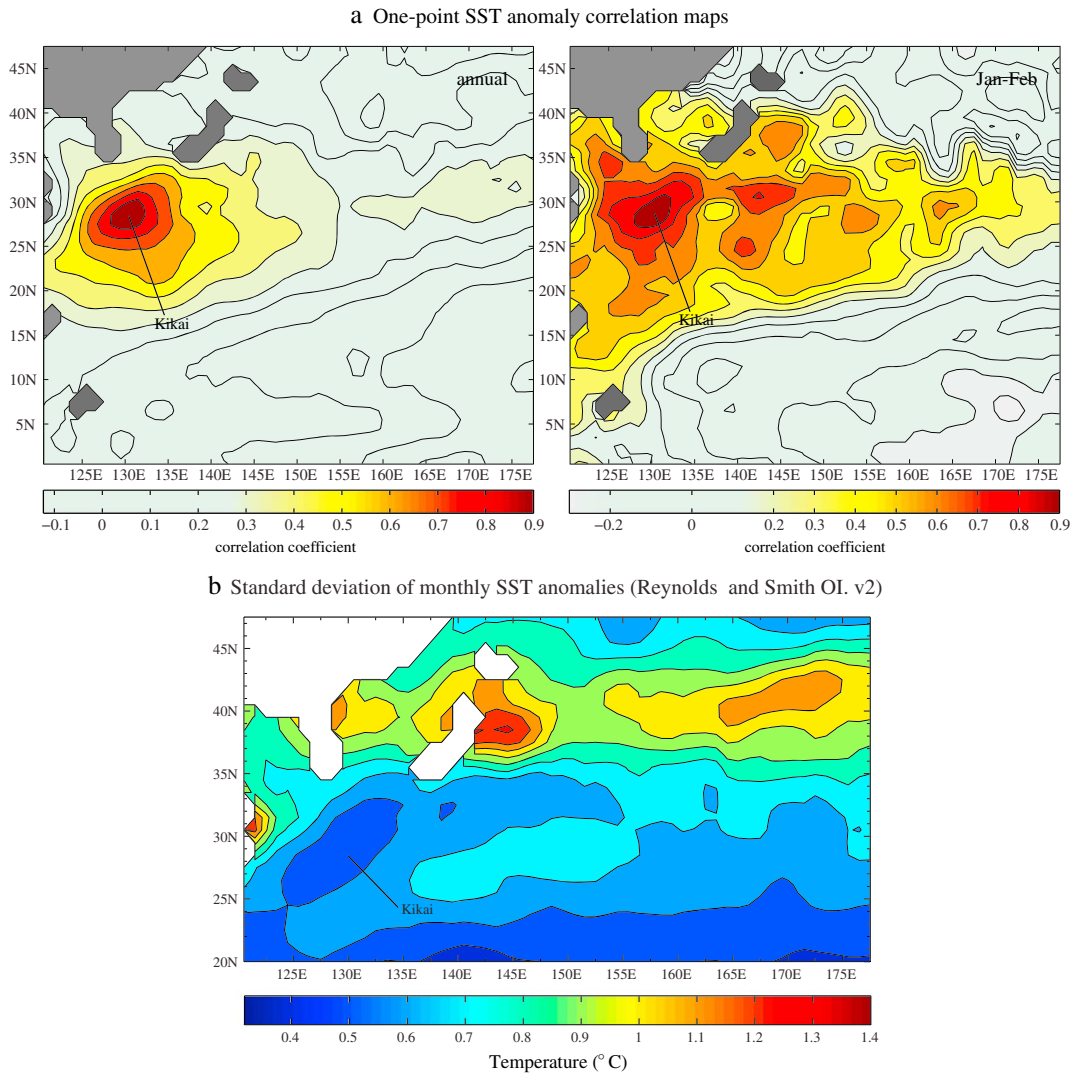


**Figure 2.** (a) The 1-point correlation maps of SST anomaly between Kikai and the northwest Pacific, calculated using 1° latitude × 1° longitude monthly data between 1982 and 2016 from NOAA OI SSTs (1971–2000 climatology) for all months (left, and January–February only (right). Note the eastward extension of the high correlation coefficient field toward the recirculation gyre in winter. (b) Based on the same data set, the standard deviation of monthly SST anomalies highlights the high variability region north of the KE (> 1°C), contrasting with lower variability (~0.5°C) along the Ryukyu Archipelago.

anomalies (+ 2°C) were also reported during summer 2001, in particular southeast of Okinawa, and shown to be associated with mesoscale eddies originating from the zonal band of high eddy kinetic energy between 20°N and 25°N (Ebuchi & Hanawa, 2003; Zhu et al., 2008). To summarize, SST variability in the KE and the southern recirculation gyre extends to the northern Ryukyu region, but anomalies related to this oceanic forcing are generally less than 0.5°C, so that it can be anticipated that corals from the Ryukyus will be best at recording anomalously strong Kuroshio advection or warm/cold eddies.

### 2.2. The Atmospheric Forcing

Both air temperature and SST in the northern Ryukyus are strongly correlated with the Western Pacific (WP) index ($r$ = 0.8, supporting information Table S1). The Arctic Oscillation (AO) has less direct influence south of 30°N (supporting information Table S1 and Figure S4). However, combined negative AO in phase with negative WP indices can force the East Asian jet stream to migrate southward and cause anomalously cold surface air temperatures in East Asia (Park & Ahn, 2016). At decadal timescale, Jhun and Lee (2004) have shown that the AO modulates the intensity of the East Asian Winter Monsoon (EAWM). Furthermore, winter SST

anomalies around Kikai and the WP and AO indices show the increase around 1988–1989 (supporting information Figure S5) that is recognized as a major regime shift in the East Asian region (Lo & Hsu, 2010; Tsunoda et al., 2008).

Although winter SSTs in southwest Japan are not strongly influenced by El Niño–Southern Oscillation (ENSO), the ENSO mode may have some influence on the WP pattern, as suggested by a correlation coefficient of 0.5 between Niño3,4 and WP indices for simultaneous winter seasons since 1951, except in 1989–1990 when the AO index was extremely positive (supporting information Table S1). The complex connection between ENSO and WP is discussed in Tanaka et al. (2016).

Spring-summer climate south of Japan is mainly controlled by solar radiation and surface heat fluxes, with lesser ocean current influence on SST, with a few exceptions as mentioned above for the summers of 1998 and 2001. Owing to the small size of the Amami-Ōshima and Kikai Islands, SST and air temperature at Naze are very similar during summer (supporting information Figure S1). Summer temperatures are influenced by the western extension of the North Pacific Subtropical High (Wu & Wang, 2015), a permanent high-pressure system of the North Pacific. Its variability is modulated by tropical air-sea interactions in the western tropical Pacific. The typical response to El Niño is a warmer following summer, ~7 months after the El Niño mature phase (Wang et al., 2000). Accordingly, annual mean SST anomalies around Kikai are weakly correlated with the Niño3,4 index averaged between October (year 0) and March (year +1) ($r$ = 0.4, supporting information Table S1), but ENSO-related anomalies are generally less than 0.5°C, except during very strong El Niño events such as in 1997/1998 or 2016/2017.

## 3. Material and Analytical Method

A 4.40 m long core was drilled in June 2009 from a large *Porites* coral colony on the south coast of Kikai (28.3°N, 130°E), near the small town of Araki. The top of the coral colony was in 3.5 m water depth. Temperature loggers were subsequently deployed at 0.5 m and 8 m water depth at the coral site, providing hourly measurements of water temperature between 2009 and 2011.

Coral preparation, laser ablation ICP-MS technique, and a calibration of coral Sr/Ca ratios with temperature for the top 15 years of coral growth have been previously described (Kawakubo et al., 2014). In short, analyses were performed at the Research School of Earth Sciences with a quadrupole ICP-MS (Varian 820-MS) equipped with an ArF excimer laser (193 nm), using a 400 μm × 40 μm rectangular slit, an energy density of ~7 J/cm$^2$, and a pulse rate of 5 Hz. The ablation is only a few microns deep. The narrow dimension of the rectangle was scanned along the growth direction of the coral at a speed of 40 μm/s. Measured isotopes include $^{11}$B, $^{25}$Mg, $^{43}$Ca, $^{55}$Mn, $^{86}$Sr, $^{137}$Ba, and $^{238}$U. The analysis of each coral slice, 6–10 cm long, was bracketed by the analysis of 3–4 mm of an in-house coral standard for calibration and to allow for instrumental drift correction, and the NIST 614 standard was added for Mn. Reproducibility of Sr/Ca ratios between successive analyses along the same track is better than 0.5%. A potentially larger source of error derives from the heterogeneity of the coral standard made from a *Porites* from Great Barrier Reef where the annual water temperature range is ~6°C. The pressed disc used in this study was thoroughly analyzed by line scans using a second disc for calibration, and vice versa. These data, once recalculated to the length of 3–4 mm commonly used for calibration, indicate an uncertainty (as standard deviation) of 0.3% for Sr/Ca ratios, equivalent to 0.5°C, and 1.8% for B/Ca, Mg/Ca, Ba/Ca, and U/Ca ratios.

## 4. Results

### 4.1. Seasonality of Coral Growth

Analyses of individual coral pieces are shown in supporting information Figure S6, including some replicate analyses made along adjacent growth axes. Overlapping sections are a critical data quality control to test the goodness of fit between successive coral pieces. When available, replicate data were averaged to provide the final Sr/Ca record (supporting information Table S2). The chronology is based on counting of the annual density bands on the positive print of the X-ray radiograph (supporting information Figure S3) and comparison with the Sr/Ca record. Screening of the coral slices under UV light (black light) further outlines the thin low-density bands deposited during winter. The base of the core is dated as summer 1578, with an uncertainty of about ±2 years, mainly related to less clear matching between pieces O3 and P1 and between Q1 and P3–P4.

Kawakubo et al. (2014) previously showed that, in spite of slower growth during the winter months, the coral Sr/Ca variations record the full annual range of water temperature. Most of the coral growth occurs in summer-autumn, which coincides with water temperatures above ~25°C and clear skies following the early-summer monsoon. The linear extension rate is generally between 8 and 10 mm per year, with a long-term increase after 1750, and particularly slow growth between 1680–1700, 1720–1730, during the 1880s, and around 1980 (supporting information Figures S3 and S6).

### 4.2. Calibration of the Coral Sr/Ca Thermometer and Assessment of Errors Associated With Reconstructed Temperatures

#### 4.2.1. Data Reduction Strategy

As a consequence of the seasonal asymmetry of coral growth, it was difficult to identify individual summer or winter months. A preliminary attempt to fit the top 10 years of a smoothed Sr/Ca record to monthly instrumental SSTs gave a calibration that underestimates the slope (sensitivity to temperature) and produces winter temperatures which are too cold. Data were first averaged to ~215–230 μm resolution, corresponding to ~10–15 days of coral skeleton linear extension. To compensate for the growth rate twice as high in summer than in winter (Kawakubo et al., 2014), data were further smoothed with a 5-point running mean to capture the narrow Sr/Ca maximum (winter) and an 11-point running mean to define the wider Sr/Ca minimum (summer). This different smoothing approach provides the best estimate for monthly minimum/maximum water temperatures in February and August SSTs, respectively. Additional smoothing for the summer maximum makes no significant difference and leaves the interpretation of the results unchanged. Annual mean temperatures were then calculated as the average of August and February values.

#### 4.2.2. Reproducibility and Problematic Sampling Paths

In this study, we have strived to minimize nonoptimal sampling of the coral skeleton and associated vital effects. However, the most recent coral skeleton pieces show some anomalously high Sr/Ca ratios (cold temperatures), in particular after 1975. Examination under scanning electron microscope of two coral pieces corresponding to the early 1960s and 1980s has revealed the presence of some scattered secondary aragonite (Kawakubo et al., 2014) that could produce the observed poor reproducibility and anomalously high Sr/Ca ratios. Ba/Ca ratios are not affected. Secondary aragonite is often grown by the coral itself as a response to an invading organism such as fungus. These infections can be related to freshwater river plumes or water pollution. Similar biases of elemental ratios caused by diagenesis have been previously reported for both living and fossil corals (Allison et al., 2007; Griffiths, 2015).

The high spatial resolution of the laser ablation ICP-MS makes this technique particularly sensitive to the sampling path selection. Suboptimal analysis paths near corallite fan margins or termination, both areas of low calcification rate, often display significant shifts of the Sr/Ca pattern, as reported before (Alibert & McCulloch, 1997; Alpert et al., 2016, their Figures S2 and S3; DeLong et al., 2013). Resulting nonclimatic Sr/Ca variations can be a major hindrance to apply spectral analysis techniques or compare proxy reconstructions to climate model simulations (e.g., Ault et al., 2013). Although the average seasonality of ~8°C is generally well captured by the Sr/Ca record, some short intervals have a suspiciously reduced range (supporting information Figure S6) and are often associated with complex coral architecture. A significant angle between the analyzed coral track and a growth vector (central axis of a corallite fan) can reduce the apparent extension rate and annual cycle, but as a result of the strongly asymmetrical shape of the Sr/Ca pattern in this subtropical coral, the winter Sr/Ca maximum will tend to be more strongly smoothed than the summer minimum. This may explain the reduced seasonality and low annual mean Sr/Ca value, hence high temperature, observed for example between 1937 and 1943. Another example of nonideal path effect on Sr/Ca ratios is shown in supporting information Figure S7 for two adjacent pieces "C4" and "C6" covering the early 1920s, with C4 not well aligned with a growth vector. The two tracks analyzed in C4 have an average Sr/Ca value systematically shifted to higher Sr/Ca ratios compared to C6 by 0.15 mmol/mol, equivalent to ~2.5°C cooler temperature. Another difficult piece was "D4" (1897–1905) which necessitated five distinct tracks to extract a satisfactory composite Sr/Ca record.

#### 4.2.3. Calibration of the Sr/Ca Thermometer and Assessment of Errors

The calibration of the Sr/Ca thermometer has been limited to the best coral sections between 1918 and 2009 by excluding 17 years from 1976 to 1992, but keeping the section 1937–1943 in order to provide realistic errors. In situ measured water temperatures for 2.5 years show that the daily range of water temperature is less than 0.5°C in winter and less than 2°C in summer. In situ water temperatures were recalculated at

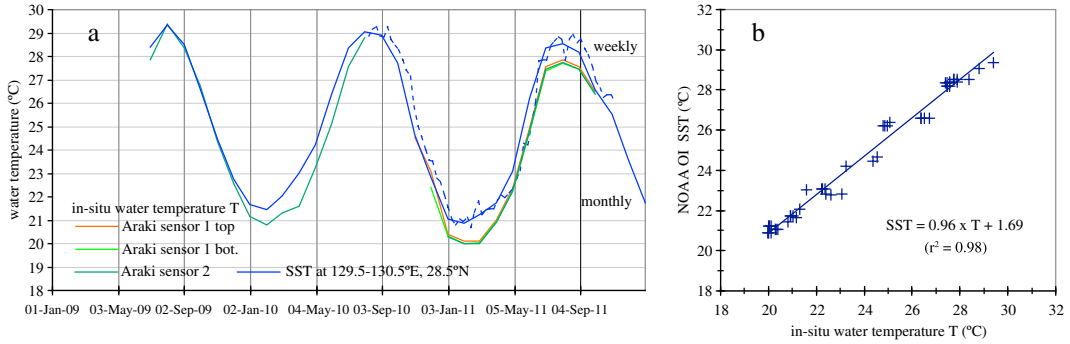


**Figure 3.** (a) Comparison between in situ measured water temperatures (monthly mean) and gridded SSTs (monthly and weekly averages from NOAA OI SSTs over 129.5°–130.5°E, 28.5°N) for the period from mid-2009 to September 2011 during which temperature sensors were deployed near Araki. (b) Linear regression between in situ and gridded SSTs. Note the ~1°C cooler in situ temperature in winter and more variable difference in summer.

monthly resolution and compared to NOAA OI SSTs (Figure 3a), suggesting ~1°C cooler waters in winter. A simple linear regression between Sr/Ca ratios and in situ water temperatures ($T$) extrapolated using the linear correlation between in situ and satellite-derived water temperatures (Figure 3b) gives the following calibration: Sr/Ca (mmol/mol) = 10.3–0.055 × $T$. This is very similar to the calibration of Sr/Ca versus in situ water temperature derived by Felis et al. (2009) for a *Porites* coral from Ogasawara, analyzed by solution high-resolution ICP-MS (Sr/Ca × $10^3$ = 10.3–0.051 × $T$). However, a small Kikai modern coral (covering 1993–1998) analyzed by Morimoto et al. (2007) produced much higher Sr/Ca ratios during winter (blue line in Figure 4a), compared to the present calibration. Since we are interested by regional rather than the local

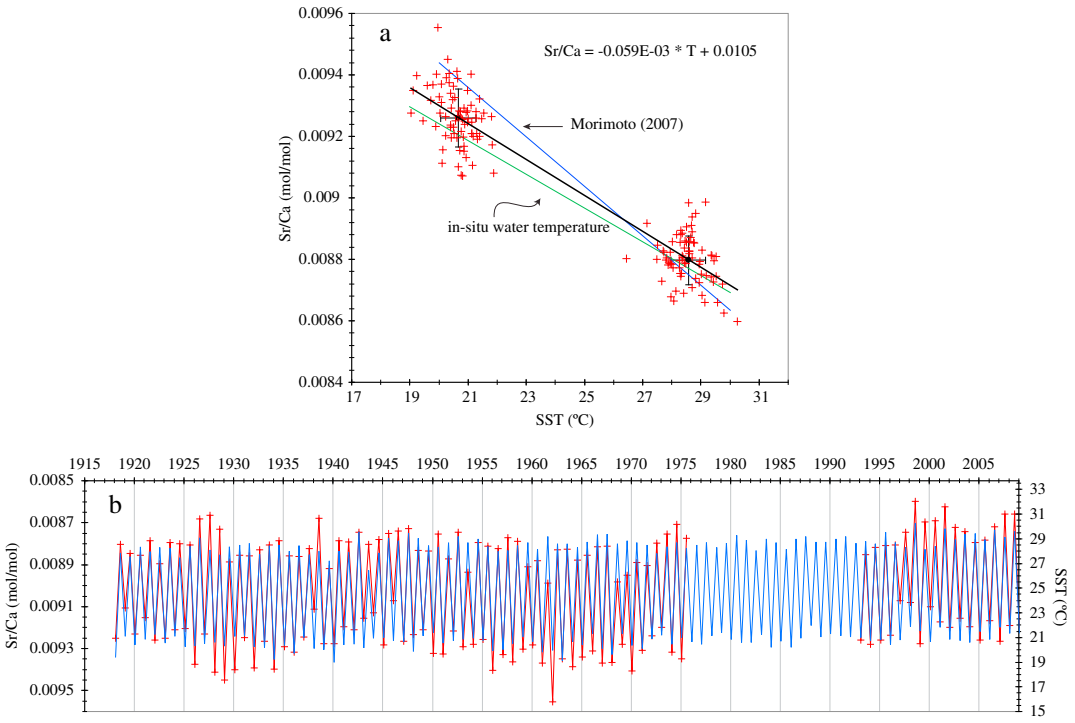


**Figure 4.** (a) Simple least squares regression between Sr/Ca minima/maxima and gridded SSTs (black line) between 1918 and 2008. Also shown are the linear regression against in situ temperature (green line) and a calibration previously reported by Morimoto et al. (2007) based on a short coral core (blue line). Error bars represent the Sr/Ca and SST interannual variations (standard deviation) for the whole period. Seasonal data for winter or for summer alone are scattered and do not define a distinct linear regression. (b) Time series showing seasonal Sr/Ca data compared with gridded SSTs (ERSST.v4 at 28°N, 130°E), with Sr/Ca scaled according to the calibration equation above. Note that the period 1976–1992 was omitted from the calibration.

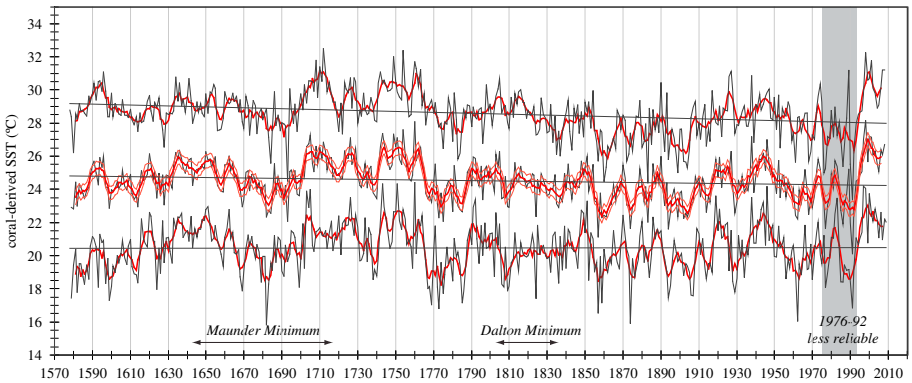


**Figure 5.** Reconstructed SST for the entire coral record, back to 1578. The upper curve is for August and the lower curve February. Each seasonal maximum/minimum is estimated to have an error of 1.2°C (1$\sigma$), as derived from the winter/summer calibration of Sr/Ca against SST. A 5 year running mean is also shown to highlight decadal variations, with an error envelope of ±0.4°C. There is no significant long-term warming or cooling, with a near-constant annual mean SST = 24.5°C ± 1.2°C. The gray rectangle indicates less reliable coral data between 1976 and 1992. Other intervals noted in supporting information Figure S6 as less reliable are of shorter duration and have been included in the 5 year running mean calculation.

water temperature of the fringing reef around Kikai, temperatures have been calibrated instead against the ERSST.v4 data set (Figure 4a) as Sr/Ca (mmol/mol) = 10.5–0.059 × *T*. As this is practically a 2-point linear regression, a first indication of errors is given by the standard deviation of the residuals between calculated and instrumental SST: 1.4°C (149 data points). A more rigorous linear regression was also implemented using a York algorithm for MATLAB (courtesy Prof. F. Albarède), taking into account errors on *x* and *y*. Using 1$\sigma$ errors of 0.3% for Sr/Ca ratios and 0.2°C for ERSST.v4 (uncertainty is in the range of 0.2–0.4°C) (Huang et al., 2015, their Figure 1), the least squares regression gives a slope of 0.0585 ± 0.0034 mmol/mol/°C and an intercept of 10.47 ± 0.09 mmol/mol (calculated errors in 2$\sigma$), and the standard deviation of the residuals between measured and adjusted Sr/Ca ratios is equivalent to 1.2°C. This value is the best estimate for the error on seasonal coral-derived temperature. If all the years between 1918 and 2009 are used for the calibration, the slope and intercept obtained by simple linear regression become 0.058 mmol/mol/°C and 10.47 mmol/mol, respectively, within errors of the parameters shown in Figure 4a. In the latter figure, the error bars represent the interannual variability, equivalent to 1.3°C for August and 1.6°C for February for coral-derived temperatures, twice higher than for instrumental SSTs (± 0.6°C for both seasons). For example, the two anomalously warm summers of 1998 and 2001 are well recorded by the coral but at ~1°C above SSTs (Figure 4b).

The entire Sr/Ca coral record is shown in Figure 5 as February and August SSTs and as annual mean SST with a 5 year running mean (red bold). Uncertainties (1$\sigma$) are estimated as

$\frac{1}{2}\sqrt{2\times1.2^2}$ = 0.8°C for annual mean SST and $\frac{0.8}{\sqrt{5}}$ ≈ 0.4°C for the 5 year running trend.

### 4.3. Coral Ba/Ca and Mn/Ca Ratios: Dependence on Temperature and Terrestrial Inputs

In order to determine the nature of the anthropogenic disturbances on water quality around Kikai, coral Ba/Ca and Mn/Ca ratios have also been monitored. Ba/Ca ratios record both seawater temperature and chemistry. However, the temperature dependence is very small and generally masked by the large Ba/Ca enrichment associated with river runoff (McCulloch et al., 2003) or upwelling (Ourbak et al., 2006). Ba being a nutrient-like element, subthermocline waters are typically enriched by a factor of ~2 relative to surface waters, for example, at 38°N, 144°E (Oba & Kato, 2013) or at 34°N, 142°E (Östlund et al., 1987). There is negligible river runoff around Kikai and no upwelling east of the Ryukyus. Upwelling is only known on the shelf off northeast Taiwan (e.g., Chen et al., 2015). Owing to the large annual range of SST, the small Ba/Ca variations in the coral skeleton reflect mostly water temperature, as shown by covariations between Ba/Ca and Sr/Ca for the two representative pieces A7 (top of the core) and N4 (circa 1690) in Figure 6. The sensitivity of Ba/Ca ratios to temperature has been derived using the calibration of Sr/Ca

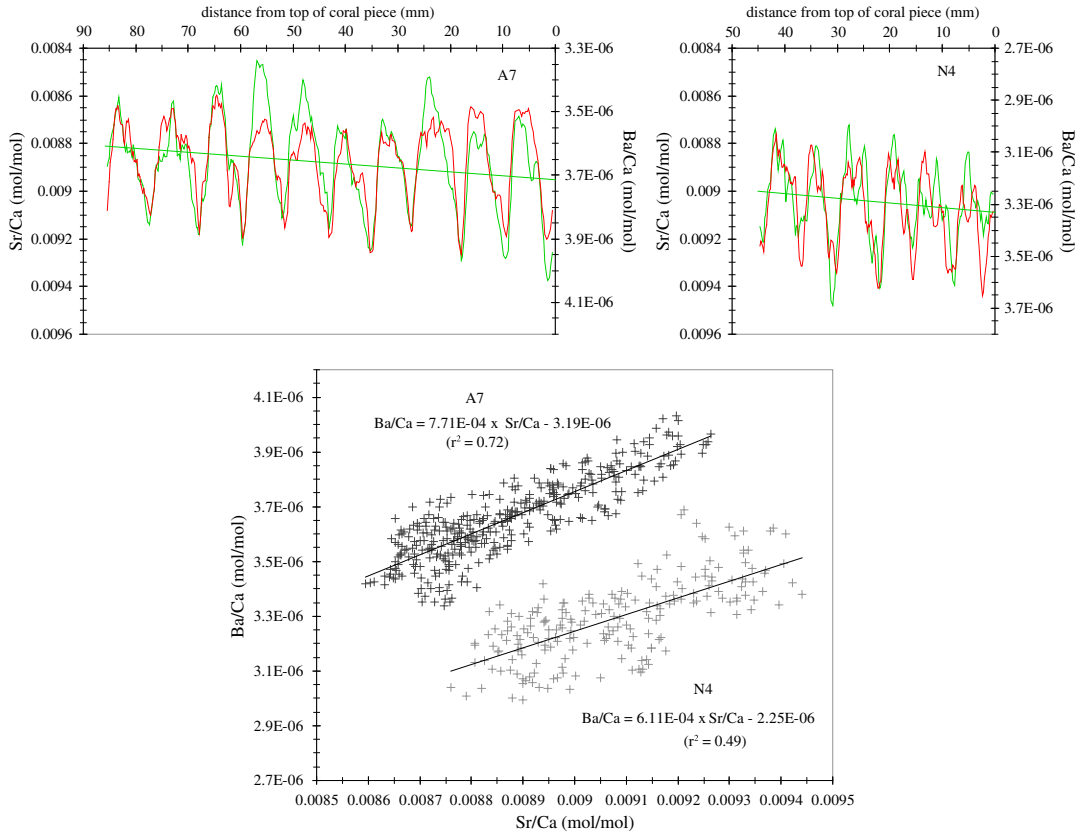


**Figure 6.** (top) Covariations between Ba/Ca (green) and Sr/Ca (red) versus distance (mm) for two coral pieces A7 (top of the core) and N4 (circa 1690) covering the warmest and coldest parts of the record, respectively. The higher Ba/Ca during the recent decades is likely to reflect some minor terrestrial inputs. (bottom) Linear regressions for the same data. See Table 1 for regression parameters obtained from some other coral pieces.

ratios against in situ water temperature. An average slope of 0.00038 (± 1) mol/mol Ba/Ca per °C is thus obtained using 13 coral pieces (Table 1). The corresponding long-term average Sr/Ca, equivalent to 24.5°C, corresponds to Ba/Ca = 3.4 ± 0.1 μmol/mol (supporting information Figure S8). There is only a slight increase to ~3.6 μmol/mol after 1983. The section between 2,800 and 2,400 mm below top of coral (1714–1760 Common Era) stands out by its lower Ba/Ca ratio, consistent with relatively low Sr/Ca (above average SST). Assuming typical open ocean seawater concentrations of 35 nmol/kg for Ba and 10.2 mmol/kg for Ca, a partition coefficient $K_D^{Ba/Ca} = Ba/Ca_{coral}/Ba/Ca_{SW} \approx 1$ can be calculated. This is slightly less than the value of 1.5 predicted by the experiments at 25°C by Dietzel et al. (2004) for inorganic aragonite precipitation and significantly less than the value of 2.1 obtained by Gaetani and Cohen (2006). Our estimate is more consistent with recent in situ measurements in both coral and seawater by LaVigne et al. (2016). The seasonal temperature variations derived from Ba/Ca variations are, however, more "noisy" compared to Sr/Ca or U/Ca ratios, limiting its use as proxy SST in the subtropics.

Some occasional Mn enrichment (Mn/Ca ≥ 0.2 μmol/mol) during the early 1920s and between 1983 and 1991 (supporting information Figure S8) occurs mainly in spring (between 1983 and 1991), with some additional occurrences in summer (e.g., 1678, 1797, 1920s, and 1986). The rest of the coral record shows very low Mn/Ca ratio in the range of 4–6 μmol/mol, close to the analytical detection limit, with seasonal variations inversely proportional to Ba/Ca, that is, higher Mn/Ca ratio in summer.

## 5. Discussion

### 5.1. Anthropogenic and Natural Environmental Disturbances

In this study, we have been attentive to natural and anthropogenic disturbances that can be recorded as chemical tracers in the coral skeleton. In the previous section, we have observed slightly higher Ba/Ca and Mn/Ca

**Table 1**
*Sr/Ca and Ba/Ca Average Molar Ratios for Individual Coral Pieces (Using the ~210–230 μm High-Resolution Data Smoothed With a 5-Point Running Mean)*

| Coral piece # | Sr/Ca (mol/mol) | Ba/Ca × $10^{-6}$ (mol/mol) | Ba/Sr (mol/mol) |
|---|---|---|---|
| A1 | 0.009010 | 3.59 | 0.000399 |
| A7 | 0.008873 | 3.66 | 0.000412 |
| A2 | 0.008975 | 3.56 | 0.000397 |
| A4 | 0.008996 | 3.46 | 0.000385 |
| B2 | 0.09057 | 3.44 | 0.000380 |
| B3 | 0.009010 | 3.41 | 0.000378 |
| B4 | 0.009012 | 3.36 | 0.000373 |
| B7 | 0.008970 | 3.47 | 0.000387 |
| D1 (October 2009) | 0.009053 | 3.35 | 0.000371 |
| D1 (1 April 2010) | 0.008874 | 3.40 | 0.000383 |
| L1 (23 September 2009) | 0.008815 | 3.16 | 0.000358 |
| L1 (28 September 2009) | 0.008929 | 3.48 | 0.000390 |
| H4 | 0.008995 | 3.39 | 0.000377 |
| N4 | 0.009077 | 3.29 | 0.000363 |
| Q2 (lines 1 and 2) | 0.008904 | 3.25 | 0.000365 |
| Average | 0.008970 | 3.42 | 0.00038 |
| Standard deviation | 0.000076 | 0.13 | 0.00001 |

*Note*. The average Ba/Sr ratio for each coral piece is the slope derived by simple linear regression between Ba/Ca and Sr/Ca.

ratios for the recent decades, indicative of minor sediment input. A similar Ba/Ca value was reported by Sowa et al. (2014) for the period 1996–2008 for a *Porites* coral from Ishigaki. The small Mn peaks are not accompanied by anomalously high Ba/Ca ratios, which may reflect differences in solubility and sources of Ba and Mn in coastal waters. Mn inputs in the coastal waters around Kikai may occur in response to agricultural land and infrastructural development, resuspension of bottom sediments during the passage of a typhoon, for example, the Mn/Ca peak at ~5 μmol/mol in summer 1990 coincides with the passage of super-Typhoon Flo, or via atmospheric deposition of anthropogenic and natural dust particles. The later could relate to the "Kosa" events or to occasional ash falls from Suwanose-jima, an active volcano 140 km north of Amami-Ōshima. Ash falls were reported there in August 2002, but no anomaly has been detected in the coral Mn/Ca ratios. The occurrence of Mn peaks in spring appears consistent with an Asian dust origin, but this warrants further investigation.

The anomalously high Sr/Ca ratios and poorly reproducible seasonal variations observed between 1976 and 1992 are consistent with the presence of scattered secondary aragonite. In the absence of major river runoff and sediment inputs, leakage of herbicides used in sugar cane fields is a possible trigger as they are known to damage symbiotic zooxantellae, and their usage became widespread in the 1970s (see supporting information). However, anomalously high elemental ratios for 1982 and 1994–2002 have also been reported in a coral growing in the more pristine environment of Ogasawara (27°N, 142°E) (Felis et al., 2009). This suggests that the biological mediation of the minor/trace element uptake from seawater may also be affected by extreme summer temperatures and by ocean acidification. There is indeed some experimental evidence of increase in the Sr/Ca ratio at 25°C at low aragonite saturation values (Cohen et al., 2009) and high seawater $pCO_2$ (Cole et al., 2016). Surface seawater pH, regularly measured in the western subtropical Pacific along the 137°E line since the early 1980s, shows a regular decrease at the high rate of −0.019 units per decade (Ishii, 2017). Furthermore, ocean acidification may be exacerbating the effects of natural acidic underground freshwater discharge at low tide, as shown by Cyronak et al. (2014) at Rarotonga (South Pacific). In situ measurements of salinity from June 1999 to December 2000 around Kikai Island by Morimoto et al. (2007) indicate a decrease from 35 in winter to 34 in summer, consistent with the maximum precipitation in early summer and subsequent freshwater discharge in the fringing reef waters. In that respect, the underground dam built in 1999, intending to limit groundwater runoff to the ocean and to secure water supply for agriculture, may have a beneficial effect on the future health of the fringing coral reef around Kikai.

### 5.2. Comparison of the Coral Record Against Instrumental SST Back to 1900

Coral-derived annual mean temperature anomalies calculated relative to the long-term average of 24.5°C ± 1.2°C (supporting information Table S2) are compared in Figures 7a and 7b to air temperature from Naze, the main town of nearby Amami-Ōshima island, and to SST using both the ERSST.v4 and HadSST3 data sets. SST anomalies at the coral site are consistent with those in the recirculation gyre dubbed "western North Pacific." Note that the *y* axis has been scaled to visually fit the larger Sr/Ca variability to instrumental SSTs. Periods of discrepancy between coral and instrumental data include the early 1900s, the second half of the 1920s, and around 1940, but instrumental data also have larger uncertainties prior to 1940. Relatively good agreement is observed between 1950 and 1975, except for winter 1962 colder in the coral (reproduced in two adjacent pieces "B3" and "B4"). Coral-derived SST anomalies for February are consistent with air temperature at Naze and SST anomalies in a similar way as for annual mean SSTs (Figures 7c and 7d). There is also good agreement with East Asia air temperature (T2m_EA) and with the WP index (Figure 8), with a correlation coefficient of 0.39 between the coral record and the WP index between 1950 and 2008, significant at the 95% level, although the correlation is best between 1950 and 1975. This lends credibility to the Sr/Ca coral record as proxy for the winter climate in the East Asian region, in particular for changes associated with the WP pattern. The Sr/Ca-derived SSTs are below average in the 1960s and decrease from 1940 to 1970. This period was

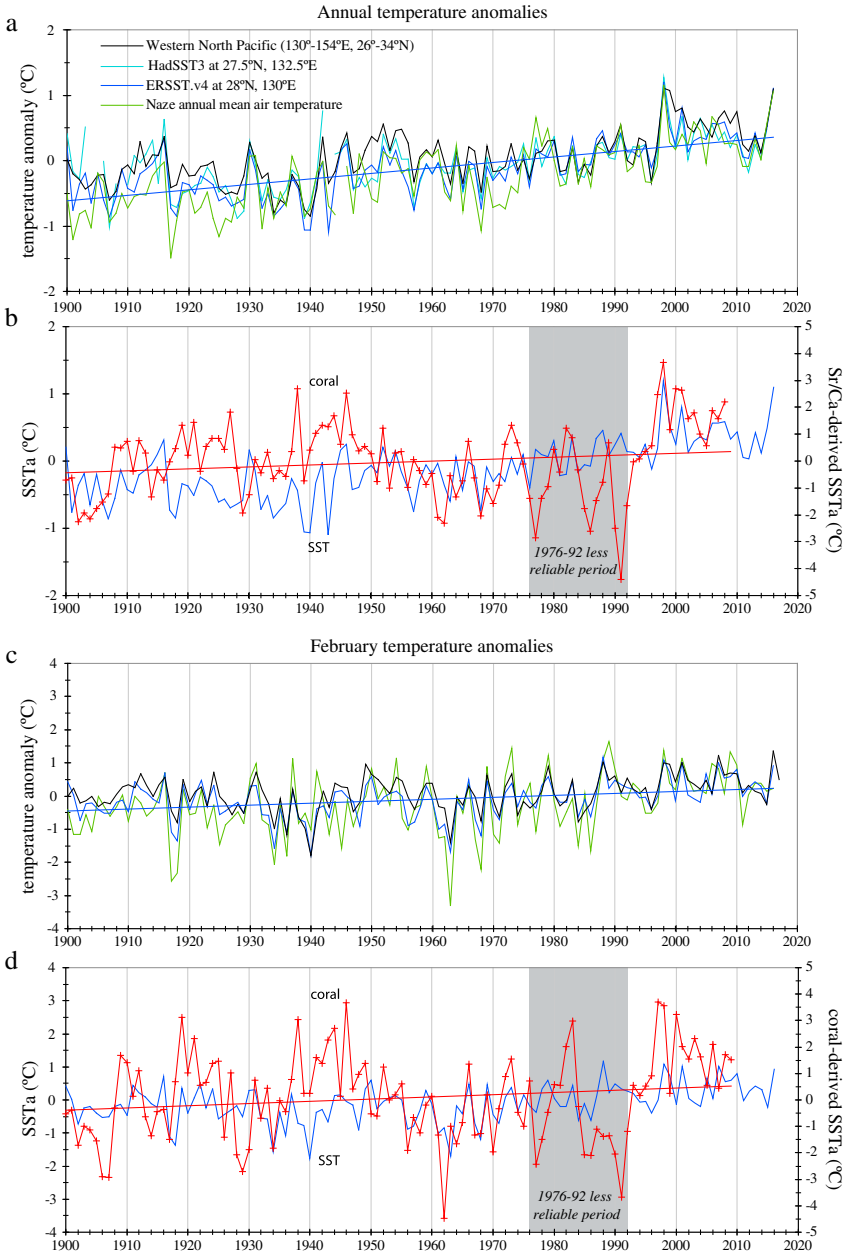


**Figure 7.** (a and b) Time series for coral-derived annual mean temperature anomalies (red) are compared to air temperatures at Naze, the main town of Amami-Ōshima (green), and to SSTs using both the ERSST.v4 (dark blue) and HadSST3 (light blue) data sets. There is good agreement between these two data sets except during the late 1920s. Also shown are SST anomalies for the larger region of the recirculation gyre (Western North Pacific, black), confirming that local gridded SSTs are representative of this larger region. The gray rectangle indicates coral data less reliable between 1976 and 1992. (c and d) For February temperature anomalies. Same legend for Figure 7c as in Figure 7a. Note the more negative temperature anomalies in winter for SAT compared to SST. There is a relatively good agreement between SAT and SST anomalies, although SAT tends to show more negative anomalies relative to SST prior to 1930 and during the early 1970s. The annual mean temperature for the 1920s is warmer in the coral record than indicated by instrumental temperatures, and this is also observed from the late 1930s to early 1940s. The long-term warming for the twentieth century is similar between the coral-derived and the instrumental SSTs and around 0.7°C per 100 years.

associated with predominantly negative WP and AO indices (supporting information Figure S5) that contributed to a stronger EAWM than average (e.g., Wang & Chen, 2014). The flattening of the warming trend in global SST during that same period is thought to have been driven for a large part by anthropogenic aerosols (Wilcox et al., 2013), the eruption of Mount Agung in 1963 adding to the

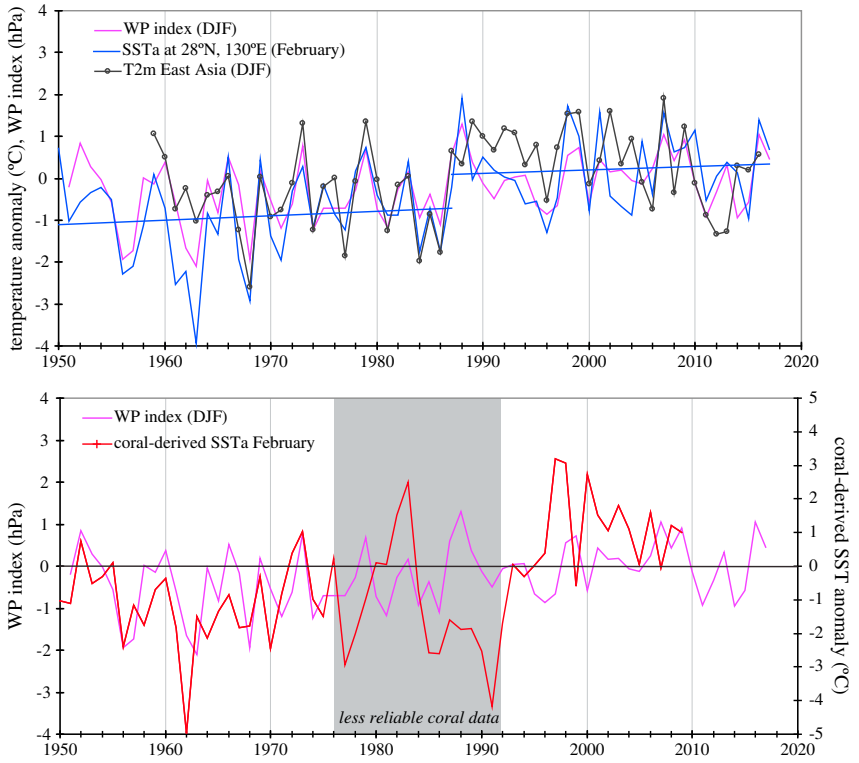


**Figure 8.** (top) Time series of SST anomalies around Kikai (ERSST.v4, standardized to the 1981–2010 period) compared to the WP index for December–January–February available back to 1950 and to the East Asian air temperatures (T2m_EA) available back to 1959. Note the shift upward in the late 1980s. (bottom) Coral-derived SST anomalies for February (red) covary with the WP index (purple) between 1950 and 1975, when the coral Sr/Ca record is most reliable.

widespread cooling in global mean temperatures from the mid-1960s to the early 1970s (Maher et al., 2015). The warming trend back to 1900 (Figure 7a) is consistent with that indicated by instrumental SST around Kikai and in the recirculation gyre region (+ 0.7°C per 100 years).

### 5.3. Possible Causes for Larger Sr-/Ca-Derived SST Variability Compared to Gridded SSTs

Larger than expected interannual and decadal variations of coral-derived temperatures are observed for the entire record back to 1578 (Figure 5), with standard deviation figures of 1.5°C for February and 1.4°C for August. Larger than expected SST anomalies in summer could be related to stress effects associated with extreme temperature. The interannual variability of summer SSTs in this region has increased since 1970, and temperature extremes ($>$ 1°C above average) can occur after strong El Niño events, as observed in 1998 and 2016 (Figure 7a). Another plausible explanation calls for more variable temperature in the shallow waters of the fringing reefs than offshore, in particular in winter when air-sea exchanges are very strong and air temperature is on average 6°C cooler than SST (supporting information Figure S1a). However, similarly large Sr/Ca anomalies have been reported for a *Porites* coral from Ogasawara (Felis et al., 2009) where air and sea surface temperatures differ only by ~2°C in winter. Here again, annual mean coral-derived SSTs have a standard deviation of 1.1°C, larger than for gridded SSTs (0.4°C). The origin of this large variability remains poorly understood. It is often attributed to vital effects or to distinct calibration slopes for seasonal and annual regressions (Alpert et al., 2016; DeLong et al., 2014; Grove et al., 2013; Wu et al., 2013). Other researchers simply disregard this problem by normalizing the annual Sr/Ca variability to that of the instrumental SST (Zinke et al., 2014). In the present study, data points for either the winter or summer, and therefore also the annual mean, do not show any statistically distinct (steeper) regression compared with the 2-point seasonal regression (Figure 4a). This suggests that the magnified Sr/Ca anomalies are largely intrinsic to the biological mediation of coral calcification. In supporting information Figure S9, 5 year smoothed data for the present record as well as three other reconstructions (Calvo et al., 2007; DeLong et al., 2007; Zinke et al., 2014) are compared

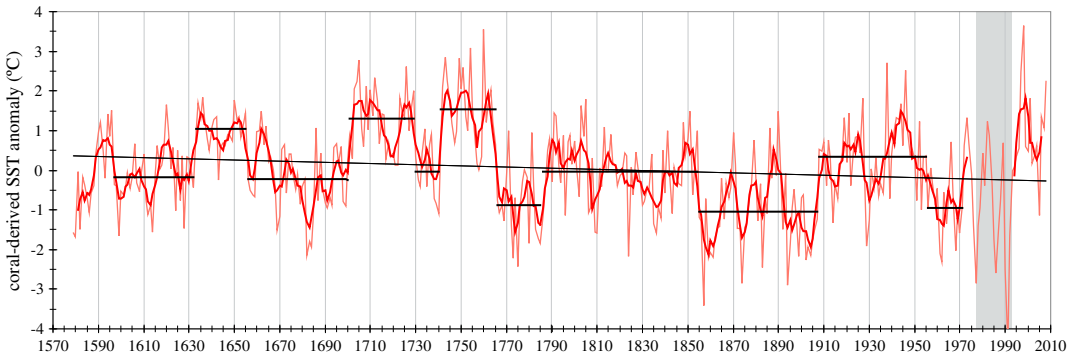


**Figure 9.** Time series of annual mean coral-derived SST anomalies (red), with a 5 year running trend (red bold) highlighting decadal to interdecadal variations. Significant regime shifts were determined using the sequential method of Rodionov (2004). Calculations were started in 1975 to avoid the less reliable coral data afterward and ended in 1578. The cut-off length $l$ = 21 years is representative of the observed interdecadal variations (15–35 years). The dates for the regime shifts are 1955, 1908, 1855, 1786, 1766, 1741, 1730, 1701, 1656, 1633, and 1597.

to instrumental SSTs at a grid centered at the coral site. The Sr/Ca-derived standard deviation is between 1.3 and 3.2 times that of instrumental SSTs. The better fit obtained for the Amédée corals by DeLong et al. (2007) may reflect their efforts to minimize vital effects by retaining only optimal sampling paths and replicating measurements on adjacent growth axes. There is also some indication that the calibration parameters may not be conservative, being slightly offset between individual fans of corallites. Supporting information Figure S10 shows the distinct linear regressions obtained for each individual coral growth axis between 1918 and 2008. The observed differences suggest that vital effects can indeed generate relatively large uncertainties in reconstructed annual SST records.

### 5.4. Decadal to Interdecadal Variability

The Sr/Ca record back to 1578 does not show any significant long-term trend, only a slightly negative trend mainly driven by decreasing summer temperatures (Figure 5). In a similar way, the large *Porites* coral colony from New Caledonia analyzed for Sr/Ca by DeLong et al. (2013) back to 1650 does not show any warming trend except for the twentieth century (+ 0.73°C). Neither does the Sr/Ca record for the Ogasawara coral analyzed by Felis et al. back to 1873 (2009, their Figure DR6). The preservation of a long-term trend demands that the Sr/Ca versus temperature relationship remains constant through time, which may be valid only within some reasonably large uncertainties, as argued above.

Prominent shifts are observed in the 5 year smoothed coral record (Figure 5), for example, a steep increase of ~1.5°C between the two 30 year periods of 1670–1700 and 1701–1730 that has been reproduced with coarser sampling and analysis by solution inductively coupled plasma atomic emission spectrometry (Kawakubo et al., 2014, their Figure 4). Other periods that stand out as below average SSTs in the coral record occur mostly in winter between 1595–1610 and 1765–1786 and for both winter and summer between 1855 and 1908. To ascertain the significance of these shifts, we have applied the statistical method of Rodionov (2004), based on a Student's $t$ test for the difference between the mean values of two subsequent regimes. The calculations (at the 95% confidence level, $p$ = 0.05) were performed backward in time, starting from 1975 to avoid the less reliable coral data afterward and ending with 1578 (Figure 9). The value for the cut-off length l was chosen as 21 years, to account for the observed interdecadal (15–35 years) variations, but similar results can be obtained for l = 21 ± 5. The average variance for running 21 year intervals is $\sigma^2$ = 0.93°C. The dates for the regime shifts are 1955, 1908, 1855, 1786, 1766, 1741, 1730, 1701, 1656, 1633, and 1597. None of these shifts coincide with a jump of the analysis path between distinct corallite fans, supporting their climatic significance. However, the amplitude of the anomalies should be interpreted with caution. Based on the large body of air temperature reconstructions for the Northern Hemisphere (e.g., Christiansen & Ljungqvist, 2012), it is questionable whether the period between 1700 and 1765 was warmer than between 1900 and 1950 by as much as 0.5°C. There is clearly a need for additional climate proxies covering the eighteenth century in the East Asian region. The Ishigaki "Tsunami

Boulders" deposited during the 1771 earthquake (Araoka et al., 2013) could provide valuable coral proxy data to compare with the present record.

Frequency analysis of the coral-derived annual or February SST anomalies between 1578 and either 1900 or 2008 (supporting information Figure S11), using the Multitaper Method (kSpectra Toolkit, three tapers, resolution = 2), shows significant power (exceeding the 95% confidence level) at the ENSO-like frequencies around 4–6 years. Low-frequency periodicity such as the ~46 years associated with the leading multidecadal mode for the North Pacific (Pacific Decadal Oscillation (PDO) like) that was identified by Park and Latif (2010) in a millennium simulation, and is linked to the subtropical gyre, is not clear in the coral-derived SST spectrum. Interestingly, the frequency of 9.5 years detected in both annual and winter coral data may represent the influence of the Kuroshio southern recirculation gyre, as this frequency is also present in the KE SST spectrum (supporting information Figure S11c). Indeed, Qiu et al. (2007) have shown that SST anomalies for a larger KE band have a dominant timescale of around 10 years, and this frequency is enhanced by the SST-induced wind stress curl forcing. A largely internal oceanic origin for the KE decadal variability has also been suggested by recent modeling results (Smirnov et al., 2014). Furthermore, Frankignoul et al. (2011) found that the decadal SST variability associated with shifts of the KE and Oyashio extensions feeds back onto the large-scale atmospheric circulation, producing changes that resemble the positive/negative phase of the North Pacific Oscillation/WP pattern. In turn, the WP pattern can alter the meridional shift of the surface Aleutian Low, and subsequently, changes in the wind stress curl over the North Pacific (associated with the Pacific Decadal Oscillation or the North Pacific Gyre Oscillation) affect the SST variability in the KE region (Qiu & Chen, 2010; Seager et al., 2001; Sugimoto & Hanawa, 2009).

The influence of global warming on the Kuroshio system dynamics and on the near-surface climate (Li et al., 2017; Qiu et al., 2014; Sato et al., 2006) provides an insight on how external forcing can influence the oceanic conditions around Japan. These high-resolution atmosphere-ocean coupled models show a spin-up of the subtropical gyre, resulting in a stronger Kuroshio jet moving northward and a stronger southern recirculation gyre. However, the associated increase in SST is mostly north of 35°N. It has also been pointed out by Révelard et al. (2016) that the decadal changes of the Kuroshio, between stable (positive) and unstable (negative) states, have consequences on SSTs that are not necessarily symmetrical. For example, during the negative phase, the cold anomaly along the KE extends more westward toward the Japan coast but only a mild anomaly is found along the upstream Kuroshio path. In consequence, the SST regime shifts observed in the Kikai coral record cannot be interpreted simply in terms of changes in the Kuroshio dynamics. As found by Sato et al. (2006), SST changes are also driven by the direct forcing from the overlying atmosphere and by the phase of the AO-like mode in response to the forcing.

### 5.5. SST Variability From Little Ice Age (1550–1700) to Recovery Period (1850–1900)

The cold period between 1660 and 1700 in the coral record (Figures 5 and 9) aligns with the minimum total solar irradiance that defines the Maunder Minimum (MM) circa 1645–1715 (Steinhilber et al., 2009). Changes toward a more negative Arctic Oscillation index have been observed during the minimum phase of the 11 year sunspot cycle (e.g., Ineson et al., 2011), inferred from paleoclimate data for the MM (Shindell et al., 2001), and simulated for a "grand" solar minimum (Ineson et al., 2015). The latter model predicts an enhanced cooling in northern Eurasia, including around Japan (−0.25°C). The relatively cold winters recurring between 1650 and 1700 in the coral record are therefore consistent with this pattern. It is still not clear how the combination of volcanic and solar forcing can account for the LIA prolonged cooling, but it is recognized that repeated explosive volcanism or some internal feedback are necessary. Some studies have emphasized the influence of ocean dynamics through ENSO variability in the Pacific Ocean (Mann et al., 2009; Meehl et al., 2009). Others call for a sea ice/ocean feedback (Miller et al., 2012) or midlatitude ocean-atmosphere coupling in the oceanic frontal zones such as the Kuroshio Oyashio extension (KOE) (e.g., Kodera et al., 2016).

The cold summers in 1783 and 1784 in the coral record (two standard deviations below the 430 year mean; Figure 9) agree with historical records of extremely cold and wet summers causing rice harvest failure and the severe "Tenmei" famine between 1782 and 1785 (Mikami, 2008). This period coincides with the long-lasting 1783–1784 Laki flood lava eruption in Iceland (Chenet et al., 2005; Thordarson & Self, 2003). Climate model simulations reproduce the observed cold anomaly of up to −1.5°C observed in northern Europe and America in the winter of 1783/1784 and predict a significant cooling in East Asia, in the range of −0.5°C to −1°C over Japan (Schmidt et al., 2012). Proxy North Atlantic Oscillation (NAO) reconstructions (Luterbacher

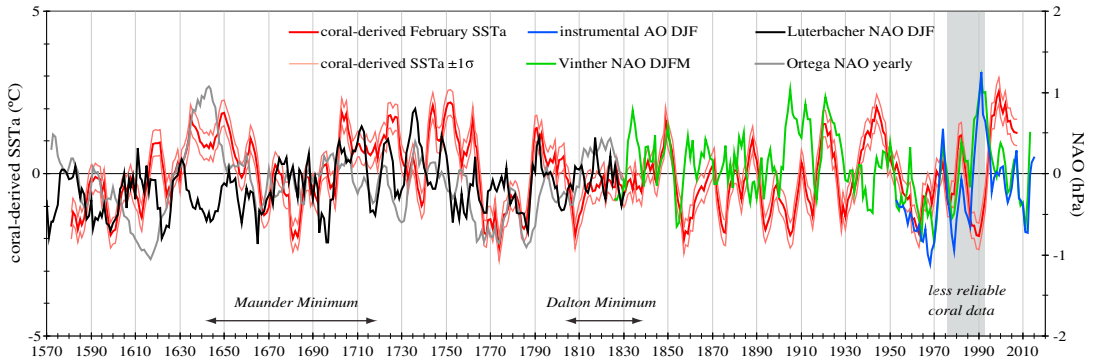


**Figure 10.** Time series of coral-derived February SST anomalies, with a 5 year running mean and 1$\sigma$ error envelope, compared to the North Atlantic Oscillation (NAO) index, also smoothed with a 5 year running average. This includes the NAO reconstructions by Luterbacher et al. (2002) (standardized relative to 1999–1950) and by Ortega et al. (2015) (their yearly model-constrained reconstruction scaled by a factor of 2/3 to compare with Luterbacher's), both shown for 1570–1830 only for clarity. Also shown are the instrumental NAO and Arctic Oscillation (AO) indices. The latter is from CPC/NOAA and is also standardized relative to the 1999–1950 base period, while the NAO index was derived from early Gibraltar and Reykjavik pressure data, back to 1823, by Vinther et al. (2003). There is good agreement between the Luterbacher and Ortega NAO reconstructions back to ~1650, but clear differences earlier.

et al., 2002; Ortega et al., 2015) also show a negative index between 1780 and 1789. Furthermore, the steep phase transitions shown by the NAO index around 1700, 1765, and 1789 are also present in the coral record. This suggests that the AO-like mode had a dominant influence on the East Asian winter climate prior to the year 1800, in a similar way as observed recently during the 1960s and since the late 1980s (He et al., 2017; Lo & Hsu, 2010).

Most simulations aimed at reproducing tree ring and ice core proxy archives find that volcanic forcing is the major driver of short-lived temperature changes in the Northern Hemisphere for the past ~1,000 years (e.g., Schneider et al., 2009; Schurer et al., 2014). Tree ring density temperature reconstructions (Neukom et al., 2014; Wilson et al., 2016) show a protracted cooling during the Dalton Minimum (circa 1807–1832) that has been related to three major explosive volcanic eruptions in 1808–1809 (unknown tropical volcano) (Guevara-Murua et al., 2014), in 1815 (Tambora) (Raible et al., 2016), and in 1835 (Cosigüina) (Longpré et al., 2014). Although the response of summer temperatures to large explosive volcanic eruptions is a coherent cooling over East Asia and the tropical ocean (Man et al., 2014), the figure obtained in these simulations for South Japan is only −0.5°C, which is within the uncertainties associated with coral-derived SSTs. In consequence, the absence of cooling after the Tambora eruption in the coral record should be interpreted with caution, while the anomalously cold winter found around 1810 is still consistent with historical reports of a particularly cold winter 1809/1810 all over Japan (Maejima & Tagami, 1986) as well as in eastern China (Hao et al., 2012).

Between 1855 and 1900, the coral indicates temperatures on average ~1°C cooler than later (1930–1957). Based on historical documents, a cool period between 1855 and 1905 has also been found in a reconstruction of winter temperatures over eastern China at the same latitude of ~30°N (Hao et al., 2012). A comparison with the Ogasawara coral record going back to 1873 (Felis et al., 2009) reveals limited consistency of decadal variations between the two corals, except during the early part of the record (1870–1895). The mid-1870s and late-1890s are particularly cold in the Kikai coral record. As the Gibraltar/Reykjavik NAO index (Vinther et al., 2003) indicates reduced atmospheric variability between 1870 and 1900 (Figure 10), and in the absence of noticeable external forcing, the SST variability shown by the coral could be driven mainly by decadal tropical variability related to ENSO. These cool intervals also coincide with two prolonged droughts in the USA in 1870–1877 and 1890–1896, which have indeed been attributed to persistent La Niña-like tropical Pacific conditions (Herweijer et al., 2006).

## 6. Conclusion

The high spatial resolution capability of laser ablation ICP-MS allows to determine precisely the Sr/Ca composition of the coral skeleton in winter, a period of much reduced coral growth, which is a significant advantage

over bulk sampling and solution analysis methods for these subtropical corals. This is particularly important in East Asia where winter temperature variations are associated with the East Asian Winter Monsoon.

With only modest interannual changes of SST expected from ocean dynamics in relation to the Kuroshio system, and being only marginally under the influence of ENSO or the Pacific Decadal Oscillation, the Ryukyus remains a challenging place for coral-based SST reconstructions. Nevertheless, the Kikai coral record shows some significant decadal to interdecadal variability, for example, colder than average temperature between 1665–1700 (coinciding with the Maunder Minimum), 1766–1788, 1855–1900, and during the 1960s and warmer than average temperature between 1700–1730, 1740–1760, 1930–1950, and since 1990. This variability is consistent with changes of SST driven by large-scale atmospheric teleconnections such as the Western Pacific and the Arctic Oscillation modes. In consequence, the coral-derived SST record reflects mainly changes in external forcing (volcanic, solar, aerosols, etc.). However, SST anomalies around Kikai Island being correlated with those in the recirculation gyre in winter, the ocean-atmosphere coupling at the Kuroshio-Oyashio confluence and extensions is likely to have some additional influence. The large-scale atmospheric circulation response to the Kuroshio extension (KE) variability at decadal to interdecadal frequencies is currently an active field of research (Frankignoul et al., 2011; O'Reilly & Czaja, 2015; Révelard et al., 2016).

**Acknowledgments**
We thank T. Ijichi, K. Kubo, and the Government of Kikaicho, Kagoshima Prefecture for logistic support during our sampling in Kikai Island. We thank H. Adachi for field assistance and Atsushi Suzuki for laboratory assistance. We are grateful to Stephen Eggins for providing access to the ICP-MS facilities at RSES and to Les Kinsley for his skillful assistance with the laser ablation ICP-MS. Joong-Bae Ahn kindly provided the time series for East Asia surface temperature based on the ERA-40 data set. Reviews by the Associate Editor Nathalie Goodwin and two anonymous reviewers were greatly appreciated. Part of this research was supported from a grant by JSPS KAKENHI (JP15KK0151 and JP17H01168) to Y. Y. Data used in this paper are provided as supporting information (Table S2).

## References

Alibert, C., & McCulloch, M. T. (1997). Strontium/calcium ratios in modern *Porites* corals from the Great Barrier Reef as a proxy for sea surface temperature: Calibration of the thermometer and monitoring of ENSO. *Paleoceanography*, *12*(3), 345–363. https://doi.org/10.1029/97PA00318

Allison, N., Finch, A. A., Webster, J. M., & Clague, D. A. (2007). Palaeoenvironmental records from fossil corals: The effects of submarine diagenesis on temperature and climate estimates. *Geochimica et Cosmochimica Acta*, *71*(19), 4693–4703. https://doi.org/10.1016/j.gca.2007.07.026

Alpert, A. E., Cohen, A. L., Oppo, D. W., DeCarlo, T. M., Gove, J. M., & Young, C. W. (2016). Comparison of equatorial Pacific sea surface temperature variability and trends with Sr/Ca records from multiple corals. *Paleoceanography*, *31*, 252–265. https://doi.org/10.1002/2015PA002897

Ammann, C. M., Joos, F., Schimel, D. S., Otto-Bliesner, B. L., & Tomas, R. A. (2007). Solar influence on climate during the past millennium: Results from transient simulations with the NCAR Climate System Model. *Proceedings of the National Academy of Sciences of the United States of America*, *104*(10), 3713–3718. https://doi.org/10.1073/pnas.0605064103

Andres, M., Park, J.-H., Wimbush, M., Zhu, X.-H., Chang, K.-I., & Ichikawa, H. (2008). Study of the Kuroshio/Ryukyu current system based on satellite-altimeter and in situ measurements. *Journal of Oceanography*, *64*(6), 937–950. https://doi.org/10.1007/s10872-008-0077-2

Araoka, D., Yokoyama, Y., Suzuki, A., Goto, K., Miyagi, K., Miyazawa, K., … Kawahata, H. (2013). Tsunami recurrence revealed by *Porites* Coral boulders in the southern Ryukyu Islands, Japan. *Geology*, *41*(8), 919–922. https://doi.org/10.1130/G34415.1

Asami, R., Yamada, T., Iryu, Y., Quinn, T. M., Meyer, C. P., & Paulay, G. (2005). Interannual and decadal variability of the western Pacific sea surface condition for the years 1787–2000: Reconstruction based on stable isotope record from a Guam coral. *Journal of Geophysical Research*, *110*, C05018. https://doi.org/10.1029/2004JC002555

Ault, T. R., Deser, C., Newman, M., & Emile-Geay, J. (2013). Characterizing decadal to centennial variability in the equatorial Pacific during the last millennium. *Geophysical Research Letters*, *40*, 3450–3456. https://doi.org/10.1002/grl.50647

Calvo, E., Marshall, J. F., Pelejero, C., McCulloch, M. T., Gagan, M. K., & Lough, J. M. (2007). Interdecadal climate variability in the Coral Sea since 1708 A.D. *Palaeogeography Palaeoclimatology Palaeoecology*, *248*(1–2), 190–201. https://doi.org/10.1016/j.palaeo.2006.12.003

Chen, C.-C., Hsu, S.-C., Jan, S., & Gong, G.-C. (2015). Episodic events imposed on the seasonal nutrient dynamics of an upwelling system off northeastern Taiwan. *Journal of Marine Systems*, *141*, 128–135. https://doi.org/10.1016/j.jmarsys.2014.07.021

Chen, T., Huang, W., & Yoon, J. (2004). Interannual variation of the East Asian cold surge activity. *Journal of Climate*, *17*(2), 401–413. https://doi.org/10.1175/1520-0442(2004)017%3C0401:IVOTEA%3E2.0.CO;2

Chenet, A.-L., Fluteau, F., & Courtillot, V. (2005). Modelling massive sulphate aerosol pollution, following the large 1783 Laki basaltic eruption. *Earth and Planetary Science Letters*, *236*(3–4), 721–731. https://doi.org/10.1016/j.epsl.2005.04.046

Christiansen, B., & Ljungqvist, F. C. (2012). The extra-tropical Northern Hemisphere temperature in the last two millennia: Reconstructions of low-frequency variability. *Climate of the Past*, *8*(2), 765–786. https://doi.org/10.5194/cp-8-765-2012

Cohen, A. L., McCorkle, D. C., de Putron, S., Gaetani, G. A., & Rose, K. A. (2009). Morphological and compositional changes in the skeletons of new coral recruits reared in acidified seawater: Insights into the biomineralization response to ocean acidification. *Geochemistry, Geophysics, Geosystems*, *10*, Q07005. https://doi.org/10.1029/2009GC002411

Cole, C., Finch, A., Hintz, C., Hintz, K., & Allison, N. (2016). Understanding cold bias: Variable response of skeletal Sr/ca to seawater $pCO_2$ in acclimated massive *Porites* corals. *Nature Science Report*, *6*, 26,888.

Cook, E. R., Krusic, P. J., Anchukaitis, K. J., Buckley, B. M., Nakatsuka, T., Sano, M., & PAGES Asia2k Members (2012). Tree-ring reconstructed summer temperature anomalies for temperate East Asia since 800 C.E. *Climate Dynamics*, *41*, 2957–2972.

Cyronak, T., Santos, I. R., Erler, D. V., Maher, D. T., & Eyre, B. D. (2014). Drivers of $pCO_2$ variability in two contrasting coral reef lagoons: The influence of submarine groundwater discharge. *Global Biogeochemical Cycles*, *28*, 398–414. https://doi.org/10.1002/2013GB004598

D'Arrigo, R., & Wilson, R. (2006). On the Asian expression of the PDO. *International Journal of Climatology*, *26*(12), 1607–1617. https://doi.org/10.1002/joc.1326

D'Arrigo, R., Wilson, R., Wiles, G., Anchukaitis, K., Solomina, O., Davi, N., … Dolgova, E. (2014). Tree-ring reconstructed temperature index for coastal northern Japan: Implications for western North Pacific variability. *International Journal of Climatology*, *35*, 3713–3720.

Davis, R. E. (1976). Predictability of sea surface temperature and sea level pressure anomalies over the North Pacific Ocean. *Journal of Physical Oceanography*, *6*(3), 249–266. https://doi.org/10.1175/1520-0485(1976)006%3C0249:POSSTA%3E2.0.CO;2

DeLong, K. L., Flannery, J. A., Poore, R. Z., Quinn, T. M., Maupin, C. R., Lin, K., & Shen, C.-C. (2014). A reconstruction of sea surface temperature variability in the southeastern Gulf of Mexico from 1734 to 2008 C.E. Using cross-dated Sr/Ca records from the coral *Siderastrea siderea*. *Paleoceanography*, *29*, 403–422. https://doi.org/10.1002/2013PA002524

DeLong, K. L., Quinn, T. M., & Taylor, F. W. (2007). Reconstructing twentieth-century sea surface temperature variability in the southwest Pacific: A replication study using multiple coral Sr/Ca records from New Caledonia. *Paleoceanography*, *22*, PA4212. https://doi.org/10.1029/2007PA001444

DeLong, K. L., Quinn, T. M., Taylor, F. W., Lin, K., & Shen, C.-C. (2012). Sea surface temperature variability in the southwest tropical Pacific since AD 1649. *Nature Climate Change*, *2*(11), 799–804. https://doi.org/10.1038/nclimate1583

DeLong, K. L., Quinn, T. M., Taylor, F. W., Shen, C.-C., & Lin, K. (2013). Improving coral-base paleoclimate reconstructions by replicating 350 years of coral Sr/Ca variations. *Palaeogeography Palaeoclimatology Palaeoecology*, *373*, 6–24. https://doi.org/10.1016/j.palaeo.2012.08.019

Dietzel, M., Gussone, N., & Eisenhauer, A. (2004). Co-precipitation of $Sr^{2+}$ and $Ba^{2+}$ with aragonite by membrane diffusion of $CO_2$ between 10 and 50°C. *Chemical Geology*, *203*(1-2), 139–151. https://doi.org/10.1016/j.chemgeo.2003.09.008

Ebuchi, N., & Hanawa, K. (2003). Influence of mesoscale eddies on variations of the Kuroshio path south of Japan. *Journal of Oceanography*, *59*(1), 25–36. https://doi.org/10.1023/A:1022856122033

Felis, T., Suzuki, A., Kuhnert, H., Dima, M., Lohmann, G., & Kawahata, H. (2009). Subtropical coral reveals abrupt early-twentieth century freshening in the western North Pacific Ocean. *Geology*, *37*(6), 527–530. https://doi.org/10.1130/G25581A.1

Frankignoul, C., Sennéchael, N., Kwon, Y., & Alexander, M. A. (2011). Influence of the meridional shifts of the Kuroshio and the Oyashio extensions on the atmospheric circulation. *Journal of Climate*, *24*(3), 762–777. https://doi.org/10.1175/2010JCLI3731.1

Fukunaka, K., & Oshiro, T. (1983). Economic development and changes in traditional farming in Okinawa. *Science Bulletin College of Agriculture University of Ryukyus*, *30*, 125–136.

Gaetani, G. A., & Cohen, A. L. (2006). Element partitioning during precipitation of aragonite from seawater: A framework for understanding paleoproxies. *Geochimica et Cosmochimica Acta*, *70*(18), 4617–4634. https://doi.org/10.1016/j.gca.2006.07.008

Griffiths, N. B. (2015). Evaluation of the effect of diagenetic cements on element/ca ratios in aragonitic early Miocene (~16 ma) Caribbean corals: Implications for 'deep-time' palaeoenvironmental reconstructions. PhD thesis, University of London.

Grove, C. A., Kasper, S., Zinke, J., Pfeiffer, M., Garbe-Schönberg, D., & Brummer, G.-J. A. (2013). Confounding effects of coral growth and high SST variability on skeletal Sr/ca. Implications for coral paleothermometry. *Geochemistry, Geophysics, Geosystems*, *14*, 1277–1293. https://doi.org/10.1002/ggge.20095

Guevara-Murua, A., Williams, C. A., Hendy, E. J., Rust, A. C., & Cashman, K. V. (2014). Observations of a stratospheric aerosol veil from a tropical volcanic eruption in December 1808: Is this the unknown ~1809 eruption? *Climate of the Past*, *10*(5), 1707–1722. https://doi.org/10.5194/cp-10-1707-2014

Hao, Z.-X., Zheng, J.-Y., Ge, Q.-S., & Wang, W.-C. (2012). Winter temperature variations over the middle and lower reaches of the Yangtze River since 1736 A.D. *Climate of the Past*, *8*(3), 1023–1030. https://doi.org/10.5194/cp-8-1023-2012

He, S., Gao, Y., Li, F., Wang, H., & He, Y. (2017). Impact of Arctic Oscillation on the East Asian climate: A review. *Earth Science Reviews*, *164*, 48–62. https://doi.org/10.1016/j.earscirev.2016.10.014

Herweijer, C., Seager, R., & Cook, E. R. (2006). North American droughts of the mid to late nineteenth century: A history, simulation and implication for Mediaeval drought. *The Holocene*, *16*(2), 159–171. https://doi.org/10.1191/0959683606hl917rp

Hong, C., & Li, T. (2009). The extreme cold anomaly over Southeast Asia in February 2008: Roles of ISO and ENSO. *Journal of Climate*, *22*(13), 3786–3801. https://doi.org/10.1175/2009JCLI2864.1

Hu, D. X., Wu, L. X., Cai, W. J., Sen Gupta, A., Ganachaud, A., Qiu, B., … Kessler, W. S. (2015). Pacific western boundary currents and their roles in climate. *Nature*, *522*(7556), 299–308. https://doi.org/10.1038/nature14504

Huang, B., Thorne, P., Smith, T., Liu, W., Lawrimore, J., Banzon, V., … Menne, M. (2015). Further exploring and quantifying uncertainties for extended Reconstructed Sea Surface Temperature (ERSST) version 4 (v4). *Journal of Climate*, *29*, 3119–3142.

Ichikawa, H., Nakamura, H., Nishina, A., & Higashi, M. (2004). Variability of northeastward current southeast of northern Ryukyu Islands. *Journal of Oceanography*, *60*(2), 351–363. https://doi.org/10.1023/B:JOCE.0000038341.27622.73

Ichikawa, K. (2001). Variation of the Kuroshio in the Tokara Strait induced by meso-scale eddies. *Journal of Oceanography*, *57*(1), 55–68. https://doi.org/10.1023/A:1011174720390

Ineson, S., Maycock, A. C., Gray, L. J., Scaife, A. A., Dunstone, N. J., Harder, J. W., … …Wood, R. A. (2015). Regional climate impacts of a possible future grand solar minimum. *Nature Communications*, *6*, 7535. https://doi.org/10.1038/ncomms8535

Ineson, S., Scaife, A. A., Knight, J. R., Manners, J. C., Dunstone, N. J., Gray, L. J., & Haigh, J. D. (2011). Solar forcing of winter climate variability in the Northern Hemisphere. *Nature Geoscience*, *4*(11), 753–757. https://doi.org/10.1038/ngeo1282

Ishii, M. (2017). Trend of ocean acidification for the past three decades in the western North Pacific subtropical zone in the western equatorial Pacific warm pool. The 9th GEOSS Asia-Pacific Symposium, Tokyo, Japan.

Jhun, J. G., & Lee, E. J. (2004). A new East Asian winter monsoon index and associated characteristics of the winter monsoon. *Journal of Climate*, *17*(4), 711–726. https://doi.org/10.1175/1520-0442(2004)017%3C0711:ANEAWM%3E2.0.CO;2

Jones, R. (2005). The ecotoxicological effects of photosystem II herbicides on corals. *Marine Pollution Bulletin*, *51*(5-7), 495–506. https://doi.org/10.1016/j.marpolbul.2005.06.027

Kaneshiro, A., Fujimura, H., Oomori, T., Gima, S., Suzuki, Y., Casareto, B. E., … Sagawa, T. (2011). Effects of herbicides on coral and seasonal distribution in water and sediments collected from rivers and coral reefs of the Ryukyu Archipelago, Japan. *American Geophysical Union*, Fall Meeting 2011, Abstract B13C-0582.

Kawakubo, Y., Yokoyama, Y., Suzuki, A., Okai, T., Alibert, C., Kinsley, L., & Eggins, S. (2014). Precise determination of Sr/Ca by laser ablation ICP-MS compared to ICP-AES and application to multi-century temperate corals. *Geochemical Journal*, *48*(2), 145–152. https://doi.org/10.2343/geochemj.2.0295

Kennedy, J. J. (2014). A review of uncertainty in in-situ measurements and datasets of sea surface temperature. *Reviews of Geophysics*, *52*, 1–32. https://doi.org/10.1002/2013RG000434

Kitada, Y., Kawahata, H., Suzuki, A., & Oomori, T. (2008). Distribution of pesticides and bisphenol A in sediments collected from rivers adjacent to coral reefs. *Chemosphere*, *71*(11), 2082–2090. https://doi.org/10.1016/j.chemosphere.2008.01.025

Kodera, K., Thiéblemont, R., Yukimoto, S., & Matthes, K. (2016). How can we understand the global distribution of the solar cycle signal on the Earth's surface? *Atmospheric Chemistry and Physics*, *16*(20), 12925–12944. https://doi.org/10.5194/acp-16-12925-2016

LaVigne, M., Grottoli, A. G., Palardy, J. E., & Sherrell, R. M. (2016). Multi-colony calibrations of coral Ba/Ca with a contemporaneous in situ seawater barium record. *Geochimica et Cosmochimica Acta*, *179*, 203–216. https://doi.org/10.1016/j.gca.2015.12.038

Li, R., Jing, Z., Chen, Z., & Wu, L. (2017). Response of the Kuroshio Extension path state to near-term global warming in CMIP5 experiments with MIROC4h. *Journal of Geophysical Research, Oceans*, *122*, 2871–2883. https://doi.org/10.1002/2016JC012468

Lim, Y.-K., & Kim, H.-D. (2013). Impact of the dominant large-scale teleconnections on winter temperature variability over East Asia. *Journal of Geophysical Research: Atmospheres*, *118*, 7835–7848. https://doi.org/10.1002/jgrd.50462

Lo, T.-T., & Hsu, H.-H. (2010). Change in the dominant decadal patterns and the late 1980s abrupt warming in the extratropical Northern Hemisphere. *Atmospheric Science Letters*, *11*(3), 210–215. https://doi.org/10.1002/asl.275

Longpré, M.-A., Stix, J., Burkert, C., Hansteen, T., & Kutterolf, S. (2014). Sulfur budget and global climate impact of the A.D. 1835 eruption of Cosigüina volcano, Nicaragua. *Geophysical Research Letters*, *41*, 6667–6675. https://doi.org/10.1002/2014GL061205

Luterbacher, J., Xoplaki, E., Dietrich, D., Jones, P. D., Davies, T. D., Portis, D., … Wanner, H. (2002). Extending North Atlantic Oscillation reconstructions back to 1500. *Atmospheric Science Letters*, *2*, 114–124.

Maejima, I., & Tagami, Y. (1986). Climatic change during historical times in Japan: Reconstruction from climatic hazard records. *Geograph. Rep. Tokyo Metr. Uni.*, *21*, 157–171.

Maher, N., McGregor, S., England, M. H., & Sen Gupta, A. (2015). Effects of volcanism on tropical variability. *Geophysical Research Letters*, *42*, 6024–6033. https://doi.org/10.1002/2015GL064751

Man, W., Zhou, T., & Jungclaus, J. H. (2014). Effects of large volcanic eruptions on global summer climate and East Asian Monsoon changes during the last millennium: Analysis of MPI-ESM simulations. *Journal of Climate*, *27*(19), 7394–7409. https://doi.org/10.1175/JCLI-D-13-00739.1

Mann, M. E., Zhang, Z., Rutherford, S., Bradley, R. S., Hughes, M. K., Shindell, D., … Ni, F. (2009). Global signatures and dynamical origins of the Little Ice Age and Medieval Climate Anomaly. *Science*, *326*(5957), 1256–1260. https://doi.org/10.1126/science.1177303

McCormack, G. (1999). From the sea that divides to the sea that links: Contradictions of ecological and economic development in Okinawa. *Capitalism Nature Socialism*, *10*(1), 3–39. https://doi.org/10.1080/10455759909358846

McCulloch, M., Fallon, S., Wyndham, T., Hendy, E., Lough, J., & Barnes, D. (2003). Coral record of increased sediment flux to the inner Great Barrier Reef since European settlement. *Nature*, *421*(6924), 727–730. https://doi.org/10.1038/nature01361

Meehl, G. A., Arblaster, J. M., Matthes, K., Sassi, F., & van Loon, H. (2009). Amplifying the Pacific climate system response to a small 11 year solar cycle forcing. *Science*, *325*(5944), 1114–1118. https://doi.org/10.1126/science.1172872

Mikami, T. (2008). Climatic variations in Japan reconstructed from historical documents. *Weather*, *63*(7), 190–193. https://doi.org/10.1002/wea.281

Miller, G. H., Geirsdóttir, Á., Zhong, Y., Larsen, D. J., Otto-Bliesner, B. L., Holland, M. M., … Thordarson, T. (2012). Abrupt onset of the Little Ice Age triggered by volcanism and sustained by sea-ice/ocean feedbacks. *Geophysical Research Letters*, *39*, L02708. https://doi.org/10.1029/2011GL050168

Miyazawa, Y., Murakami, H., Miyama, T., Varlamov, S. M., Guo, X., Waseda, T., & Sil, S. (2013). Data assimilation of the high-resolution sea surface temperature obtained from the Aqua-Terra satellites (MODIS-SST) using an ensemble Kalman filter. *Remote Sensing*, *5*(6), 3123–3139. https://doi.org/10.3390/rs5063123

Morimoto, M., Kayanne, H., Abe, O., & McCulloch, M. T. (2007). Intensified mid-Holocene Asian monsoon recorded in corals from Kikai Island, subtropical northwestern Pacific. *Quaternary Research*, *67*(02), 204–214. https://doi.org/10.1016/j.yqres.2006.12.005

Nakai, T., & Oki, K. (2004). Status of coral reefs around the country: Amami Archipelago. In *Coral Reefs of Japan* (pp. 172–174). Tokyo, Japan: Ministry of the Environment (Ed.)

Neukom, R., Gergis, J., Karoly, D. J., Wanner, H., Curran, M., Elbert, J., … Frank, D. (2014). Inter-hemispheric temperature variability over the past millennium. *Nature Climate Change*, *4*(5), 362–367. https://doi.org/10.1038/nclimate2174

Oba, T. & Kato, Y. (2013). Section profile of barium along 47°N in the North Pacific from the 15KH-12-4 Cruise. Annual Meeting of the Geochemical Society of Japan 2013, https://doi.org/10.14862/geochemproc.60.0.203.0.

Ohyama, M., Yonenobu, H., Choi, J.-N., Park, W.-K., Hanzawa, M., & Suzuki, M. (2013). Reconstruction of northeast Asia spring temperature 1784-1990. *Climate of the Past*, *9*(1), 261–266. https://doi.org/10.5194/cp-9-261-2013

O'Reilly, C. H., & Czaja, A. (2015). The response of the Pacific storm track and atmospheric circulation to Kuroshio Extension variability. *Quarterly Journal of the Royal Meteorological Society*, *141*(686), 52–66. https://doi.org/10.1002/qj.2334

Ortega, P., Lehner, F., Swingedouw, D., Masson-Delmotte, V., Raible, C. C., Casado, M., & Yiou, P. (2015). A model-tested North Atlantic Oscillation reconstruction for the past millennium. *Nature*, *523*(7558), 71–74. https://doi.org/10.1038/nature14518

Östlund, H. G., Craig, H., Broecker, W. S., & Spencer, D. (1987). Atlantic, Pacific, and Indian Ocean expeditions, shorebased data and graphics. In *International decade of ocean exploration* (Vol. 7, 200 pp.). Washington, DC: NSF. hdl:10013/epic.43023.d001

Ourbak, T., Corrège, T., Malaizé, B., Le Cornec, F., Charlier, K., & Peypouquet, J. P. (2006). A high-resolution investigation of temperature, salinity, and upwelling activity proxies in corals. *Geochemistry, Geophysics, Geosystems*, *7*, Q03013. https://doi.org/10.1029/2005GC001064

Park, H. J., & Ahn, J. B. (2016). Combined effect of the Arctic Oscillation and the Western Pacific pattern on East Asia winter temperature. *Climate Dynamics*, *46*(9-10), 3205–3221. https://doi.org/10.1007/s00382-015-2763-2

Park, W., & Latif, M. (2010). Pacific and Atlantic multidecadal variability in the Kiel Climate Model. *Geophysical Research Letters*, *37*, L24702. https://doi.org/10.1029/2010GL045560

Qiu, B. (2000). Interannual variability of the Kuroshio Extension system and its impact on the wintertime SST field. *Journal of Physical Oceanography*, *30*(6), 1486–1502. https://doi.org/10.1175/1520-0485(2000)030%3C1486:IVOTKE%3E2.0.CO;2

Qiu, B., & Chen, S. (2010). Eddy-mean flow interaction in the decadally modulating Kuroshio Extension system. *Deep-Sea Research Part II*, *57*(13-14), 1098–1110. https://doi.org/10.1016/j.dsr2.2008.11.036

Qiu, B., Chen, S., & Schneider, N. (2014). A coupled decadal prediction of the dynamic state of the Kuroshio Extension system. *Journal of Climate*, *27*(4), 1751–1764. https://doi.org/10.1175/JCLI-D-13-00318.1

Qiu, B., Schneider, N., & Chen, S. (2007). Coupled decadal variability in the North Pacific: An observationally constrained idealized model. *Journal of Climate*, *20*(14), 3602–3620. https://doi.org/10.1175/JCLI4190.1

Raible, C. C., Brönnimann, S., Auchmann, R., Brohan, P., Frölicher, T. L., Graf, H.-F., … Wegmann, M. (2016). Tambora 1815 as a test case for high impact volcanic eruptions: Earth system effects. *WIREs Climate Change*, *7*(4), 569–589. https://doi.org/10.1002/wcc.407

Révelard, A., Frankignoul, C., Sennéchael, N., Kwon, Y., & Qiu, B. (2016). Influence of the decadal variability of the Kuroshio Extension on the atmospheric circulation in the cold season. *Journal of Climate*, *29*(6), 2123–2144. https://doi.org/10.1175/JCLI-D-15-0511.1

Reynolds, R. W., Rayner, N. A., Smith, T. M., Stokes, D. C., & Wang, W. (2002). An improved in situ and satellite SST analysis for climate. *Journal of Climate*, *15*(13), 1609–1625. https://doi.org/10.1175/1520-0442(2002)015%3C1609:AIISAS%3E2.0.CO;2

Rodionov, S. N. (2004). A sequential algorithm for testing climate regime shifts. *Geophysical Research Letters*, *31*, L09204. https://doi.org/10.1029/2004GL019448

Rogers, J., & McHugh, M. (2002). On the separability of the North Atlantic oscillation and Arctic oscillation. *Climate Dynamics*, *19*, 599–608.

Sakashita, W., Yokoyama, Y., Miyahara, H., Yamaguchi, Y. T., Aze, T., Obrochta, S. P., & Nakatsuka, T. (2016). Relationship between early summer precipitation in Japan and the El Niño-Southern and Pacific Decadal Oscillations over the past 400 years. *Quaternary International*, *397*, 300–306. https://doi.org/10.1016/j.quaint.2015.05.054

Sakuno, Y., & Oki, K. (2015). Relationship between turbid water and coral damage distribution using ALOS AVNIR-2 images and diving survey data immediately after the heavy rain disaster of the Amami-Ōshima Island, Japan. *Advances in Remote Sensing*, *04*(01), 25–34. https://doi.org/10.4236/ars.2015.41003

Sato, Y., Yukimoto, S., Tsujino, H., Ishizaki, H., & Noda, A. (2006). Response of North Pacific ocean circulation in a Kuroshio-resolving ocean model to an Arctic Oscillation (AO)-like change in Northern Hemisphere atmospheric circulation due to greenhouse-gas forcing. *Journal of the Meteorological Society of Japan*, *84*(2), 295–309. https://doi.org/10.2151/jmsj.84.295

Schmidt, A., Thordarson, T., Oman, L. D., Robock, A., & Self, S. (2012). Climatic impact of the long-lasting 1783 Laki eruption: Inapplicability of mass-independent sulfur isotopic composition measurements. *Journal of Geophysical Research*, *117*, D23116. https://doi.org/10.1029/2012JD018414

Schneider, D. P., Ammann, C. M., Otto-Bliesner, B. L., & Kaufman, D. S. (2009). Climate response to large, high-latitude and low-latitude volcanic eruptions in the Community Climate System Model. *Journal of Geophysical Research*, *114*, D15101. https://doi.org/10.1029/2008JD011222

Schurer, A., Tett, S., & Hegerl, G. (2014). Small influence of solar variability on climate over the past millennium. *Nature Geoscience*, *7*, 104–108.

Seager, R., Kushnir, Y., Naik, N. H., Cane, M. A., & Miller, J. (2001). Wind-driven shifts in the latitude of the Kuroshio–Oyashio extension and generation of SST anomalies on decadal timescales. *Journal of Climate*, *14*, 4149–4165.

Sheikh, M. A., Oomori, T., Fujimura, H., Higuchi, T., Imo, T., Akamatsu, A., … Yasumura, S. (2012). Distribution and potential effects of novel antifouling herbicide Diuron on coral reefs. In R. Alvarez-Fernandez (Ed.), *Herbicides—Environmental Impact Studies and Management Approaches* (pp. 83–94). InTech. Retrieved from http://www.intechopen.com

Shindell, D. T., Schmidt, G. A., Mann, M. E., Rind, D., & Waple, A. (2001). Solar forcing of regional climate change during the Maunder Minimum. *Science*, *294*(5549), 2149–2152. https://doi.org/10.1126/science.1064363

Smirnov, D., Newman, M., & Alexander, M. A. (2014). Investigating the role of ocean–atmosphere coupling in the North Pacific ocean. *Journal of Climate*, *27*(2), 592–606. https://doi.org/10.1175/JCLI-D-13-00123.1

Sowa, K., Watanabe, T., Kan, H., & Yamano, H. (2014). Influence of land development on Holocene *Porites* coral calcification at Nagura Bay, Ishigaki Island, Japan. *PLoS One*, *9*(2), e88790. https://doi.org/10.1371/journal.pone.0088790

Steinhilber, F., Beer, J., & Fröhlich, C. (2009). Total solar irradiance during the Holocene. *Geophysical Research Letters*, *36*, L19704. https://doi.org/10.1029/2009GL040142

Sugimoto, S., & Hanawa, K. (2009). Decadal and interdecadal variations of the Aleutian low activity and their relation to upper oceanic variations over the North Pacific. *Journal of the Meteorological Society of Japan*, *87*(4), 601–614. https://doi.org/10.2151/jmsj.87.601

Suzuki, A., Kawahata, H., Tanimoto, Y., Tsukamoto, H., Gupta, P., & Yukino, I. (2000). Skeletal isotopic record of a *Porites* coral during the 1998 mass bleaching event. *Geochemical Journal*, *34*(4), 321–329. https://doi.org/10.2343/geochemj.34.321

Tanaka, S., Nishii, K., & Nakamura, H. (2016). Vertical structure and energetics of the Western Pacific teleconnection pattern. *Journal of Climate*, *29*(18), 6597–6616. https://doi.org/10.1175/JCLI-D-15-0549.1

Thompson, D. W. J., & Wallace, J. M. (1998). The Arctic Oscillation signature in the wintertime geopotential height and temperature fields. *Geophysical Research Letters*, *25*(9), 1297–1300. https://doi.org/10.1029/98GL00950

Thoppil, P. G., Metzger, E. J., Hurlburt, H. E., Smedstad, O. M., & Ichikawa, H. (2016). The current system east of the Ryukyu Islands as revealed by a global ocean reanalysis. *Progress in Oceanography*, *141*, 239–258. https://doi.org/10.1016/j.pocean.2015.12.013

Thordarson, Th., & Self, S. (2003). Atmospheric and environmental effects of the 1783–1784 Laki eruption: A review and reassessment. *Journal of Geophysical Research*, *108*(D1), 4011. https://doi.org/10.1029/2001JD002042

Tierney, J. E., Abram, N. J., Anchukaitis, K. J., Evans, M. N., Giry, C., Kilbourne, K. H., … Zinke, J. (2015). Tropical sea surface temperatures for the past four centuries reconstructed from coral archives. *Paleoceanography*, *30*, 226–252. https://doi.org/10.1002/2014PA002717

Tomita, H., Kubota, M., Cronin, M. F., Iwasaki, S., Konda, M., & Ichikawa, H. (2010). An assessment of surface heat fluxes from J-OFURO2 at the KEO and JKEO sites. *Journal of Geophysical Research*, *115*, C03018. https://doi.org/10.1029/2009JC005545

Trenberth, K. E., & Paolino, D. A. (1980). The Northern Hemisphere sea-level pressure dataset: Trends, errors and discontinuities. *Monthly Weather Review*, *108*(7), 855–872. https://doi.org/10.1175/1520-0493(1980)108%3C0855:TNHSLP%3E2.0.CO;2

Tsunoda, T., Kawahata, H., Suzuki, A., Minoshima, K., & Shikazono, N. (2008). East Asian monsoon to El Niño/Southern Oscillation: A shift in the winter climate of Ishigaki Island accompanying the 1988/1989 regime shift, based on instrumental and coral records. *Geophysical Research Letters*, *35*, L13708. https://doi.org/10.1029/2008GL033539

Urban, F. E., Cole, J. E., & Overpeck, J. T. (2000). Influence of mean climate change on climate variability from a 155-year tropical Pacific coral record. *Nature*, *407*(6807), 989–993. https://doi.org/10.1038/35039597

Vinther, B. M., Andersen, K. K., Hansen, A. W., Schmith, T., & Jones, P. D. (2003). Improving the Gibraltar/Reykjavik NAO index. *Geophysical Research Letters*, *30*(23), 2222. https://doi.org/10.1029/2003GL018220

Wallace, J. M., & Gutzler, D. S. (1981). Teleconnections in the geopotential height field during the Northern Hemisphere winter. *Monthly Weather Review*, *109*(4), 784–812. https://doi.org/10.1175/1520-0493(1981)109%3C0784:TITGHF%3E2.0.CO;2

Wang, B., Wu, R., & Fu, X. (2000). Pacific-East Asia teleconnection: How does ENSO affect East Asian climate? *Journal of Climate*, *13*(9), 1517–1536. https://doi.org/10.1175/1520-0442(2000)013%3C1517:PEATHD%3E2.0.CO;2

Wang, L., & Chen, W. (2014). An Intensity Index for the East Asia winter monsoon. *Journal of Climate*, *27*(6), 2361–2374. https://doi.org/10.1175/JCLI-D-13-00086.1

Wilcox, L. J., Highwood, E. J., & Dunstone, N. J. (2013). The influence of anthropogenic aerosol on multi-decadal variations of historical global climate. *Environmental Research Letters*, *8*(2). https://doi.org/10.1088/1748-9326/8/2/024033

Wilson, R., Anchukaitis, K., Briffa, K. R., Büntgen, U., Cook, E., D'Arrigo, R., … Zorita, E. (2016). Last millennium northern hemisphere summer temperatures from tree rings: Part I: The long term context. *Quaternary Science Reviews*, *134*, 1–18. https://doi.org/10.1016/j.quascirev.2015.12.005

Wischow, D. (1999). Sr/Ca- und U/Ca-Thermometrie an Korallen (*Porites lutea*) aus dem Indischen Ozean. PhD diss., University of Göttingen, Germany.

Wu, H. C., Linsley, B. K., Dassié, E. P., Schiraldi, B., & deMenocal, P. B. (2013). Oceanographic variability in the South Pacific Convergence Zone region over the last 210 years from multi-site coral Sr/Ca records. *Geochemistry, Geophysics, Geosystems*, *14*, 1435–1453. https://doi.org/10.1029/2012GC004293

Wu, L., & Wang, C. (2015). Has the Western Pacific Subtropical High extended westward since the late 1970s? *Journal of Climate*, *28*(13), 5406–5413. https://doi.org/10.1175/JCLI-D-14-00618.1

Yamaguchi, M. (1986). *Acanthaster planci* infestations of reefs and coral assemblages in Japan: A retrospective analysis of control efforts. *Coral Reefs*, *5*(1), 23–30. https://doi.org/10.1007/BF00302168

Yamaguchi, Y. T., Yokoyama, Y., Miyahara, H., Sho, K., & Nakatsuka, T. (2010). Synchronized northern hemisphere climate change and solar magnetic cycles during the Maunder Minimum. *PNAS*, *107*(48), 20,697–20,702. https://doi.org/10.1073/pnas.1000113107

Yokochi, H. (2004). Coral reef disturbances: Predation damage to corals. In *Coral reefs of Japan* (pp. 49–55). Tokyo, Japan: Ministry of the Environment.

Yu, L. S., & Weller, R. A. (2007). Objectively analyzed air-sea heat fluxes for the global ice-free oceans (1981–2005). *Bulletin of the American Meteorological Society*, *88*(4), 527–539. https://doi.org/10.1175/BAMS-88-4-527

Zhang, Y., Sperber, K. R., & Boyle, J. S. (1997). Climatology and interannual variation of the East Asian Winter Monsoon: Results from the 1979–95 NCEP/NCAR reanalysis. *Monthly Weather Review*, *125*(10), 2605–2619. https://doi.org/10.1175/1520-0493(1997)125%3C2605:CAIVOT%3E2.0.CO;2

Zhu, X., Park, J. H., & Huang, D. (2008). Observation of baroclinic eddies southeast of Okinawa Island. *Science in China Series D: Earth Sciences*, *51*(12), 1802–1812. https://doi.org/10.1007/s11430-008-0146-9

Zinke, J., Rountrey, A., Feng, M., Xie, S.-P., Dissard, D., Rankenburg, K., … McCulloch, M. T. (2014). Corals record long-term Leeuwin Current variability during Ningaloo Niño/Niña since 1795. *Nature Communications*, *5*, 3607. https://doi.org/10.1038/ncomms4607